SISSA

Supermassive primordial black holes from inflation

View the article online for updates and enhancements.

You may also like

Supermassive primordial black holes from inflation

Dan Hooper,[a,b,c] **Aurora Ireland,**[d] **Gordan Krnjaic**[a,b,c] **and Albert Stebbins**[c]

[a]*Kavli Institute for Cosmological Physics, University of Chicago,*
Chicago, IL, U.S.A.

[b]*Department of Astronomy and Astrophysics, University of Chicago,*
Chicago, IL, U.S.A.

[c]*Theoretical Astrophysics Group, Fermi National Accelerator Laboratory,*
Batavia, IL, U.S.A.

[d]*Department of Physics, University of Chicago,*
Chicago, IL, U.S.A.

E-mail: dhooper@fnal.gov, anireland@uchicago.edu, krnjaicg@fnal.gov,
stebbins@fnal.gov

ABSTRACT: There is controversy surrounding the origin and evolution of our universe's largest supermassive black holes (SMBHs). In this study, we consider the possibility that some of these black holes formed from the direct collapse of primordial density perturbations. Since the mass of a primordial black hole is limited by the size of the cosmological horizon at the time of collapse, these SMBHs must form rather late, and are naively in conflict with constraints from CMB spectral distortions. These limits can be avoided, however, if the distribution of primordial curvature perturbations is highly non-Gaussian. After quantifying the departure from Gaussianity needed to evade these bounds, we explore a model of multi-field inflation — a non-minimal, self-interacting curvaton model — which has all the necessary ingredients to yield such dramatic non-Gaussianities. We leave the detailed model building and numerics to a future study, however, as our goal is to highlight the challenges associated with forming SMBHs from direct collapse and to identify features that a successful model would need to have. This study is particularly timely in light of recent observations of high-redshift massive galaxy candidates by the James Webb Space Telescope as well as evidence from the NANOGrav experiment for a stochastic gravitational wave background consistent with SMBH mergers.

Contents

1 Introduction

Supermassive black holes (SMBHs) are ubiquitous in our universe, being present in the centers of nearly all massive galaxies. Quasars,[1] powered by black holes with masses $M \sim 10^{8-10}\,M_\odot$, are also found in large numbers in the high-redshift universe. At present, over 170 quasars have been observed at $z > 6$, with the most distant at $z = 7.54$, and several hundred others at $z = 5 - 6$ [2–10]. Figure 1 shows the quasar abundance as a function of redshift over several ranges of black hole mass. While this magnitude limited quasar catalog is believed to be nearly complete out to $z \sim 5$, only a small fraction of SMBHs are, in fact, quasars. A more complete census of SMBHs is possible in the local universe where one finds $\Omega_{\rm SMBH}(z=0) \sim 10^{-6}$ [11]. This contrasts with the peak quasar mass density of $\Omega_{\rm quasar}(z=2) \sim 10^{-8}$. While specific models for SMBH population evolution have been proposed [12–14], the limited available data leaves a great deal of uncertainty.

---

[1]Quasars are the most luminous active galactic nuclei (AGN). In this paper, quasar refers to an AGN that is sufficiently luminous to appear in a quasar catalog such as SDSS DR7 [1]. While this definition is redshift-dependent, the most luminous quasars should be consistently present in the catalog up to the DR7 redshift limit of 5. In the text, the phrase "quasar mass" refers to the mass of the black hole that powers the quasar.

It is usually assumed that SMBHs grow over time from relatively low-mass seeds (possibly the remnants of Population III stars [15]) through the process of accretion. The rate of mass accretion is Eddington limited to

$$\dot{M}_{\text{Edd}} \lesssim \frac{M_{\text{BH}}}{\tau_S}, \tag{1.1}$$

where

$$\tau_{\text{S}} = \frac{\varepsilon\,\sigma_{\text{T}}}{4\pi\,G\,m_{\text{p}}} \approx 45\ \text{Myr}\left(\frac{\varepsilon}{0.1}\right) \tag{1.2}$$

is the Salpeter time [16], $\sigma_{\text{T}} = 8\pi\,\alpha^2/(3m_e^2)$ is the Thomson cross section, m_p is the proton mass, and ε is the radiative efficiency. At the Eddington-limited rate, a $10^2\,M_\odot$ black hole seed would require $\sim 0.8\,\text{Gyr}$ to grow to $M \sim 10^{10}\,M_\odot$. Since $z \sim 6\text{--}7$ corresponds to only $\sim 0.7\text{--}0.9\,\text{Gyr}$ after the Big Bang, such a scenario would require these large high-redshift black holes to have grown at high accretion rates almost continuously throughout the first Gyr of our universe's history. Interestingly, there seems to be quite a significant population of quasars at $z \sim 6$ to 7 in this mass range [4, 17–19].

The continuous accretion required to explain this rapid growth contrasts with the intermittent accretion observed of SMBHs at lower redshifts. Further, from figure 1 we see that the most massive $M_{\text{BH}} \gtrsim 10^{10}\,M_\odot$ population has remained approximately constant since at least $z \sim 5$ [20]. This would require any growth in the number of SMBHs to be balanced by a decrease in the fraction of SMBHs that are actively quasars. From this perspective, it is surprising that so many highly-massive quasars have been observed at such high redshifts [21–25]. These observations prompt two intriguing questions:

1. If these quasars grew from small black hole seeds, how did they come to be so massive on such a short timescale?

2. Why did their growth rate dramatically slow down during the subsequent 13 Gyr?

Various solutions to the first question have been put forth, including an enhanced role of mergers as well as the possibility of super-Eddington accretion [26]. However frequent mergers would require more heavily clustered populations in the early universe, and further can have both positive and negative impacts on SMBH growth, since they can also kick SMBHs out of the material-rich centers of galaxies. A certain degree of super-Eddington growth is expected to occur in high-redshift galaxies containing large reservoirs of gas and efficient angular momentum transport due to turbulence. However as increased accretion produces powerful jets and outflows which drive material away, it is uncertain how long it can be sustained. Feedback effects from transient periods of super-Eddington growth are actually expected to impede SMBH growth within a few Myr [27].

Regarding the second question, it has been suggested that the suppressed growth of the most massive black holes after the first Gyr could perhaps be attributed to galaxy-scale feedback. This, however, would require the M-σ relation[2] to evolve with redshift and for the quasar luminosity function to steepen at the highest values [28, 29]. Alternatively, it has been proposed that there might be a maximum mass that black holes can reach through

---

[2]The M-σ relation is the observed correlation between the velocity dispersion of a stellar bulge σ and the mass of the SMBH at its center.
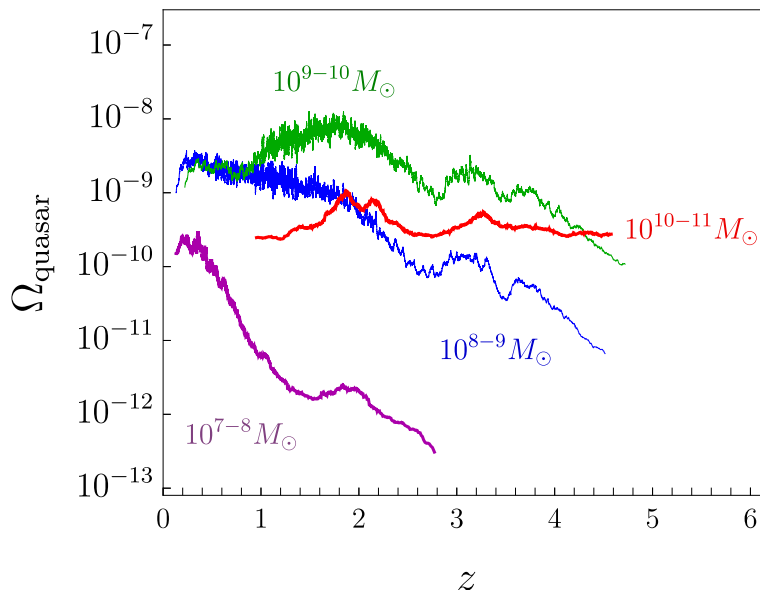
Figure 1. Estimates of the quasar black hole comoving mass density in units of the $z = 0$ critical density as a function of redshift, plotted for the four different mass classes indicated. Black hole masses and redshifts are taken from the DR7 SDSS quasar survey [1], which covers 20% of the sky and the redshift range $0 < z < 5$. The results shown represent the moving average of 100 quasars sorted by redshift.

accretion, resulting from the fragmentation of the accretion disks that could have otherwise facilitated rapid black hole growth [30]. Despite these suggestions, there remain many open questions concerning the origin and evolution of our universe's most massive black holes.

In this study, we take these questions to motivate another possibility: that our universe's most massive black holes did not acquire most of their mass through accretion, but are instead predominantly primordial in origin.[3] Unlike the small primordial black holes (PBH) typically considered as dark matter candidates, these massive objects would have formed at "late" times, as governed by the size of the cosmological horizon. During the radiation dominated era, the horizon contains the following amount of energy:

$$M_H = \frac{4\pi}{3} \rho R_H^3 \approx 3 \times 10^9 \, M_\odot \left(\frac{10 \, \text{keV}}{T} \right)^2 \left(\frac{3.36}{g_\star(T)} \right)^{1/2} , \qquad (1.3)$$

where $R_H = H^{-1}$ is the size of the horizon, $\rho = \pi^2 g_\star(T) T^4/30$ is the radiation density, and $g_\star$ is the number of relativistic species at temperature T. When a sufficiently large density fluctuation collapses to form a PBH,[4] the mass of the resulting black hole is typically

---

[3]Primordial black holes (PBHs) have previously been considered as SMBH seeds [31]. Unlike population III stars, which do not form until $z \sim 30-20$, PBH seeds form much earlier, and so the timing problem is allayed. Refs. [32, 33] have argued that establishing a population of PBHs with mass $10^2-10^6 M_\odot$ by $z \sim 20$ would be sufficient to seed even the most massive SMBHs. Here we consider the more exotic possibility of SMBHs from direct collapse, with little growth through accretion required.

[4]There exist other PBH formation mechanisms beyond the collapse of overdensities seeded by inflation. For example, PBH could form during first order cosmological phase transitions [34] or due to the collapse of supercritical vacuum bubbles nucleated during inflation [35]. The prospect of primordial SMBHs from these mechanisms is discussed in ref. [36] and ref. [37], respectively.

an order one fraction of the horizon mass, $M_{\mathrm{BH}} \simeq \gamma M_H$, where $\gamma \sim 0.2$ quantifies the efficiency of collapse [38]. From eq. (1.3), we conclude that the PBHs in the mass range of interest here form after the start of Big Bang nucleosynthesis ($T \sim \mathrm{MeV}$ corresponds to $M_H \sim 10^5 \, M_\odot$) but well before the onset of matter domination or recombination ($T \sim \mathrm{eV}$ corresponds to $M_H \sim 3 \times 10^{17} \, M_\odot$).

Many inflationary models enable PBHs to form efficiently [39], including those in which the inflaton undergoes a period of ultra-slow-roll [40–43], or whose potential features localized bumps, dips, or steps on small scales [44–46]. More generically, a local enhancement of the power spectrum $\mathcal{P}_\zeta$ requires a deviation from slow-roll evolution (see for example, refs. [47–61]). Regardless of the mechanism, PBH formation requires a significant enhancement in the amplitude of the primordial power spectrum. Assuming Gaussian statistics, this amplitude must be $\mathcal{P}_\zeta(k_{\mathrm{BH}}) \sim 10^{-2}$, seven orders of magnitude larger than observed on large scales, $\mathcal{P}_\zeta(k_{\mathrm{CMB}}) \simeq 2.1 \times 10^{-9}$ [62]. Such an amplification inevitably leads to large CMB spectral distortions. In particular, for scales $k_{\mathrm{BH}} \lesssim 10^5 \, \mathrm{Mpc}^{-1}$, corresponding to black holes in the mass range $M_{\mathrm{BH}} \gtrsim 10^3 M_\odot$, the predicted spectral distortions are in strong conflict with COBE/FIRAS measurements [63, 64].

In principle, PBHs can form from smaller peaks in the power spectrum if the tail of the ζ distribution is sufficiently non-Gaussian. Of course, observations on large scales and measurements of the non-linearity parameters f_{NL} and g_{NL} seem to indicate that ζ is very nearly Gaussian on CMB scales [65, 66]. However the scales on which PBHs are formed can be disconnected from CMB scales, and so these bounds need not apply.

In this paper, we quantify the degree of non-Gaussianity that would be required to viably produce primordial SMBHs and present a model of inflation that contains the necessary features. We begin in section 2 by reviewing the calculation of the PBH abundance in the Press-Schechter formalism. In section 3, we examine how measurements of spectral distortions constrain the primordial power spectrum, and demonstrate that the appreciable formation of SMBHs from Gaussian density fluctuations is excluded on the basis of these constraints. Section 4 considers departures from Gaussianity, and quantifies the heaviness of the distribution needed to evade these bounds. In section 5, we review the calculation of the curvature perturbation and its statistics in the standard curvaton scenario, which has been shown to be capable of producing appreciable non-Gaussianity. This model, however, cannot viably produce a significant abundance of primordial SMBHs, so in section 6 we introduce self-interactions to augment the non-Gaussianity and speculate on the maximum PBH abundance in this model. We conclude in section 7 with a discussion of our results and some comments on directions for future investigations.

2   Primordial black holes from Gaussian perturbations

The initial abundance of PBHs is quantified in terms of their mass fraction at the time of formation:

$$\beta \equiv \frac{\rho_{\mathrm{BH}}}{\rho_{\mathrm{tot}}} \,. \tag{2.1}$$

For PBHs that formed during radiation domination, this quantity is related to the fractional energy density in black holes today, $\Omega_{\mathrm{BH}} \simeq \beta \, (1 + z_f) \, \Omega_R$, where z_f is the redshift at the

time of black hole formation. Using eq. (1.3) and entropy conservation, this can be written more conveniently in terms of the initial PBH mass as:

$$\Omega_{\rm BH} \simeq 10^{-6} \left(\frac{\beta}{10^{-10}}\right) \left(\frac{\gamma}{0.2}\right)^{1/2} \left(\frac{10^8\,M_\odot}{M_{\rm BH}}\right)^{1/2} \left(\frac{g_{\star,s}(T_f)}{3.91}\right)^{1/3} \left(\frac{3.36}{g_\star(T_f)}\right)^{1/4} , \qquad (2.2)$$

where T_f is the temperature at the time of black hole formation.

In the standard[5] treatment based on the Press-Schechter formalism [72], β is computed by integrating the probability distribution P_δ for the coarse-grained density contrast $\delta = \delta\rho/\bar\rho$ over all values greater than the critical threshold for collapse, δ_c:

$$\beta \simeq 2 \int_{\delta_c}^{\infty} d\delta\, P_\delta[\delta] . \qquad (2.3)$$

The factor of 2 is customarily introduced[6] to compensate for the undercounting that otherwise arises [72]. This prescription has the benefit of having an intuitive interpretation — we are summing over the fraction of regions with a sufficient overdensity to collapse to form a PBH — and a simple implementation. One issue concerns the uncertainty[7] of the collapse threshold, which should in principle depend on the overdensity profile.[8] Assuming a spherical profile, we expect a perturbation to be able to collapse during radiation domination if the size of the overdensity at maximum expansion exceeds the Jeans length. This led to Carr's original estimate of $\delta_c = c_s^2 = 1/3$ [38], where c_s is the sound speed of density perturbations. A more careful treatment that is applicable for an arbitrary equation of state,[9] w, finds [81]:

$$\delta_c = \frac{3(1+w)}{5+3w} \sin^2\left(\frac{\pi\sqrt{w}}{1+3w}\right) , \qquad (2.4)$$

which has been shown to faithfully replicate the results of numerical simulations and yields $\delta_c = 0.414$ during radiation domination. We adopt this value throughout our analysis.

While the coarse-grained density contrast is the proper object to consider when computing the probability of PBH formation, it is often convenient to work directly with the curvature

---

[5]One can also calculate the black hole abundance using peak theory [67–70]. Unlike Press-Schechter, where the overdensity must simply exceed the threshold, peak theory further demands that it be a local maximum. This formalism has been demonstrated to be more appropriate when perturbations exist on multiple scales. As we consider a sharply peaked spectrum, the simpler Press-Schechter prescription suffices for our purposes. A comprehensive comparison can be found in [71], which demonstrated that differences are minimal so long as the window function is implemented properly.

[6]It is unclear whether this factor should still be included when considering asymmetric probability distribution functions, as in the case of non-Gaussianities. We retain it nevertheless since this is an ultimately inconsequential $\mathcal{O}(1)$ effect.

[7]It has been demonstrated that a more precise quantity which does away with this uncertainty is the compaction function $\mathcal{C}$, defined as twice the local mass excess over the comoving areal radius [73]. The value of the compaction at its peak is interpreted as the threshold. See also ref. [74].

[8]Since the overdensity profile is modified in the presence of non-Gaussianities, these can also change the threshold for collapse [75–78]. Given the uncertainties involved in these calculations, we take a conservative position and determine δ_c using eq. (2.4).

[9]It was argued in [79] that the softening of the equation of state at electron-positron annihilation should lead to an enhancement in the formation of PBHs with $M_{\rm BH} \sim 10^6 M_\odot$. However [80] pointed out that due to the onset of neutrino free-streaming, overdensities are reduced at this time, leading to an overall suppression of PBH formation.

perturbation ζ, since its statistics are more easily computed from underlying inflationary models. When large perturbations exist only on one scale, as is the case for the sharply peaked power spectra we consider, only a minimal amount of error is incurred by making this approximation. On superhorizon scales, ζ is related to the density contrast field by [82]

$$\delta = -\frac{2(1+w)}{5+3w}\left(\frac{1}{aH}\right)^2 e^{-2\zeta}\left(\nabla^2\zeta + \frac{1}{2}(\partial_i\zeta)^2\right).$$

(2.5)

Working to linear[10] order in radiation domination, this simplifies to the Fourier space relation:

$$\delta_k \simeq \frac{4}{9}\left(\frac{k}{aH}\right)^2 \zeta_k,$$

(2.6)

which implies that their power spectra, defined for arbitrary Fourier variable f_k via the 2-point function as $\langle f_k f_{k'}\rangle = \frac{2\pi^2}{k^3}\mathcal{P}_f(k)\delta^{(3)}(\vec{k}+\vec{k}')$, are related as

$$\mathcal{P}_\delta(k) \simeq \frac{16}{81}\left(\frac{k}{aH}\right)^4 \mathcal{P}_\zeta(k).$$

(2.7)

Note that at the time of horizon crossing $k \simeq aH$, when a perturbation can collapse to form a black hole,[11] the density contrast and curvature perturbation are linearly related, $\delta \simeq \frac{4}{9}\zeta$. We can then assume that peaks in δ also correspond to peaks in ζ, and work directly with the curvature perturbation. In terms of ζ, the initial abundance in the Press-Schechter formalism reads:

$$\beta \simeq 2\int_{\zeta_c}^\infty d\zeta\, P_\zeta[\zeta],$$

(2.8)

where the collapse threshold $\zeta_c \simeq \frac{9}{4}\delta_c$ follows from $\sigma_\delta^2 \simeq \frac{16}{81}\sigma_\zeta^2$, since $\mathcal{P} \sim \sigma^2$ for a sharply peaked spectrum. More precisely, the variance of ζ smoothed on the scale $R \simeq (aH)^{-1} \simeq k^{-1}$ can be computed from the power spectrum as [84]

$$\sigma_\zeta^2(R) \equiv \langle\zeta\rangle_R^2 = \int_0^\infty \frac{dk}{k}\tilde{W}^2(k,R)\mathcal{P}_\zeta(k),$$

(2.9)

where $\tilde{W}(k,R)$ is the Fourier transform of the (real space) window function used to coarse-grain δ. It is unclear what functional form for the window function most accurately reproduces the actual relation between the PBH abundance and power spectrum, but popular choices in the literature include the (volume normalized) Gaussian, as well as real and k-space top hats. For simplicity, we use the former, $\tilde{W}(k,R) = \exp\left(-k^2R^2/2\right)$, but see [85, 86] for a discussion of the resultant uncertainties.

Consider the case of a Gaussian distribution $P_\zeta = P_\zeta^G$, where

$$P_\zeta^G = \frac{1}{\sqrt{2\pi}\sigma_\zeta}e^{-\zeta^2/2\sigma_\zeta^2}.$$

(2.10)

---

[10]A certain degree of non-Gaussianity inevitably arises in the density contrast field due to this nonlinear relation. This implies that even if the statistics of ζ were perfectly Gaussian, those of δ would not be. See, for example, ref. [82] for discussion.

[11]There is additional uncertainty in the calculation of PBH abundance coming from non-linear effects around the time of horizon crossing. See ref. [83].

In this case the mass fraction at formation evaluates to

$$\beta = \text{erfc}\left(\frac{\zeta_c}{\sqrt{2}\sigma_\zeta}\right) \simeq \sqrt{\frac{2}{\pi}}\frac{\sigma_\zeta}{\zeta_c}\exp\left(-\frac{\zeta_c^2}{2\sigma_\zeta^2}\right),\qquad(2.11)$$

where erfc is the complimentary error function and the second approximation holds for $\zeta_c \gg \sigma_\zeta$, which is generically true for all cases of physical interest. Since the threshold is fixed, the initial abundance is determined solely by the variance of the power spectrum. In order to have $\beta = 10^{-20}$, we see we need $\sigma_\zeta^2 \simeq 0.01$, corresponding to a peak in the power spectrum of $\mathcal{P}_\zeta \sim 0.01$, which is 7 orders of magnitude greater than the value measured on CMB scales. Since the amplification of $\mathcal{P}_\zeta$ needed for PBH formation depends on β only logarithmically, this degree of enhancement is a generic requirement for any non-vanishing initial abundance.

3 Spectral distortions

The small scales relevant for primordial SMBH formation are well below the angular resolution probed by current CMB measurements. Nevertheless, inhomogeneities on these scales will generate isotropic deviations from the usual blackbody spectrum [87–91]. These deviations are known as spectral distortions and in this context it is useful to distinguish between three characteristic redshift intervals:

- **Thermalization era ($z > 2 \times 10^6$)**: at high redshifts, Compton scattering $\gamma e \to \gamma e$, double Compton scattering $\gamma e \to \gamma\gamma e$, and Bremsstrahlung $ep \to ep\gamma$ maintain a blackbody spectrum for the photons, and spectral distortions are exponentially suppressed.

- **μ-era ($2 \times 10^5 < z < 2 \times 10^6$)**: during this era, photon number changing processes, double Compton scattering and Bremsstrahlung, become ineffective at maintaining a blackbody spectrum. Compton scattering, however, continues to redistribute photon energies to maintain a Bose-Einstein distribution, parameterized by both a temperature, T, and a chemical potential, μ. A μ-distortion refers to a Bose-Einstein distribution with $\mu \neq 0$.

- **y-era ($z < 2 \times 10^5$)**: Compton scattering becomes ineffective at redistributing photon energies during this era, so there are no processes to maintain a Bose-Einstein distribution. Spectral distortions that are generated at these redshifts are characterized by a departure from an equilibrium distribution, and often yield so-called y-distortions.[12]

A spectrum with a (positive) y-distortion can be expressed as an average of blackbodies with slightly different temperatures [93–96]. An average of blackbodies with a mean temperature $\bar{T}$ and variance $\bar{T}^2\Delta$ will (for $\Delta \ll 1$) be a y-distorted blackbody characterized by the temperature $T = \bar{T}(1+\Delta^2)$ and the parameter $y = \Delta^2/2$. y-type distortions can be generated through a variety of mechanisms, including the Compton scattering of CMB photons with a

---

[12]Technically, the division between the two types of spectral distortions is not entirely unambiguous, and inhomogeneities dissipating around $z \sim 5 \times 10^4$ can give rise to distortions of an intermediate type, whose shape is not simply the sum of μ- and y-type distortions [92].

population of electrons with a different temperature. In this paper, we will be interested in y-distortions that are generated through photon diffusion. Limits on such spectral distortions allow us to constrain the amplitude of inhomogeneities on very small scales [97].

μ- and y-type spectral distortions are traditionally quantified in terms of the parameters μ and y, which are related to the fractional increase in energy per photon (relative to a blackbody spectrum with the same number density of photons) [87, 91]:

$$\mu \simeq 1.4 \frac{\Delta\rho_\gamma}{\rho_\gamma} \qquad \text{and} \qquad y \simeq 0.25 \frac{\Delta\rho_\gamma}{\rho_\gamma} \,. \tag{3.1}$$

By introducing k-space window functions accounting for the effects of thermalization and dissipation, μ and y can be approximately calculated from the spectrum of density perturbations, P_ζ [91, 95]:

$$\mu \simeq 2.2 \int_{k_{\min}}^{\infty} \frac{dk}{k} \mathcal{P}_\zeta(k) \left[\exp\left(-\frac{k}{5400\,\mathrm{Mpc}^{-1}} \right) - \exp\left(-\left[\frac{k}{31.6\,\mathrm{Mpc}^{-1}} \right]^2 \right) \right] \,, \tag{3.2}$$

$$y \simeq 0.4 \int_{k_{\min}}^{\infty} \frac{dk}{k} \mathcal{P}_\zeta(k) \exp\left(-\left[\frac{k}{31.6\,\mathrm{Mpc}^{-1}} \right]^2 \right) \,, \tag{3.3}$$

where $k_{\min} = 1\,\mathrm{Mpc}^{-1}$.

The strongest existing constraints on spectral distortions come from the COBE/FIRAS instrument, which restricts $|\mu| \lesssim 9.0 \times 10^{-5}$ and $|y| \lesssim 1.5 \times 10^{-5}$ at the 95% C.L. [63, 64]. The standard cosmological model predicts spectral distortions of $\mu \sim 2 \times 10^{-8}$ and $y \sim 10^{-6}$ [98], consistent with current limits. The models of interest in this study have enhanced P_ζ, and thus enhanced μ and y, which can be constrained by CMB measurements.

For concreteness, consider the case of a power spectrum that is sharply peaked at a single scale, k_{BH}:

$$\mathcal{P}_\zeta(k) = \sigma_\zeta^2 \, k \, \delta(k - k_{\mathrm{BH}}). \tag{3.4}$$

Using the delta-function to perform the integral, μ and y become functions of k_{BH} and σ_ζ^2 alone. From the horizon crossing condition $k = aH$, and fact that $H = 1.66\sqrt{g_\star(T)}T^2/M_{\mathrm{Pl}}$ during radiation domination, we can relate the wavenumber to the temperature,

$$k_{\mathrm{BH}} = 92\,\mathrm{Mpc}^{-1} \left(\frac{T}{10\,\mathrm{keV}} \right) \left(\frac{g_\star(T)}{3.36} \right)^{1/2} \left(\frac{3.91}{g_{\star,S}(T)} \right)^{1/3} \,, \tag{3.5}$$

which can then be related to the horizon mass using eq. (1.3) to estimate the mass of the resulting black hole:

$$M_{\mathrm{BH}} \simeq 5 \times 10^8 \, M_\odot \left(\frac{92\,\mathrm{Mpc}^{-1}}{k_{\mathrm{BH}}} \right)^2 \left(\frac{\gamma}{0.2} \right) \left(\frac{g_\star(T)}{3.36} \right)^{1/2} \left(\frac{3.91}{g_{\star,S}(T)} \right)^{2/3} \,. \tag{3.6}$$

For the sharply peaked spectrum of eq. (3.4), adopting $\gamma = 0.2$, and for black holes in the mass range of interest, the μ- and y-parameters can be written as

$$\mu \simeq 2.2\sigma_\zeta^2 \left\{ \exp\left[-\left(\frac{1.5 \times 10^5 \, M_\odot}{M_{\mathrm{BH}}} \right)^{1/2} \right] - \exp\left[-\left(\frac{4.5 \times 10^9 \, M_\odot}{M_{\mathrm{BH}}} \right) \right] \right\} \,, \tag{3.7}$$

$$y \simeq 0.4\sigma_\zeta^2 \exp\left[-\left(\frac{4.5 \times 10^9 \, M_\odot}{M_{\mathrm{BH}}} \right) \right] \,. \tag{3.8}$$
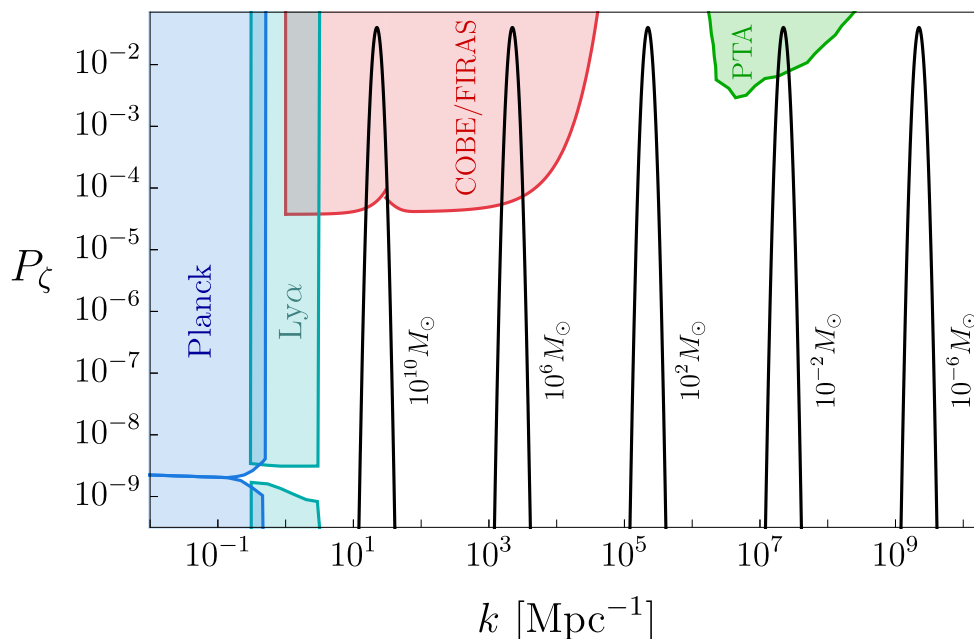
Figure 2. Constraints on the primordial power spectrum $\mathcal{P}_\zeta$ [99] coming from CMB temperature anisotropies (dark blue) [66], Lyman-α forest (light blue) [100], CMB spectral distortions (red) [63, 64], and pulsar timing arrays (green) [101]. The cusp in the COBE/FIRAS excluded region signifies the wavenumber where constraints from μ- and y-type distortions are equally restrictive. Overlaid are illustrative sharply peaked log-normal power spectra resulting in the formation of PBHs with $M_{\rm BH} = 10^{10}, 10^6, 10^2, 10^{-2}$, and $10^{-6} M_\odot$ and an initial abundance of $\beta = 10^{-20}$, assuming Gaussian statistics for ζ.

Note that these results should also hold, for example, in the case of a log-normal spectrum of sufficiently narrow width.

In eqs. (3.7) and (3.8), we can identify the impact of the various eras described earlier in this section. In particular, for $M_{\rm BH} \ll 1.5 \times 10^5 \, M_\odot$ (corresponding to $k_{\rm BH} \gg 5400/{\rm Mpc}$), the black holes are formed during the thermalization era, and both μ- and y-type spectral distortions are suppressed. For $1.5 \times 10^5 \, M_\odot \ll M_{\rm BH} \ll 4.5 \times 10^9 \, M_\odot$ ($31.6/{\rm Mpc} \lesssim k_{\rm BH} \lesssim 5400/{\rm Mpc}$), the black holes are forming during the μ-era, leading primarily to μ-type spectral distortions. Larger black holes form later, yielding primarily y-type spectral distortions.

We can use eqs. (3.7) and (3.8) to quickly estimate whether a scenario featuring primordial SMBHs is consistent with spectral distortion constraints. Recall that, for the case of Gaussian statistics, a value of $\sigma_\zeta^2 \gtrsim 10^{-2}$ is required in order to obtain a non-negligible abundance of PBHs. For such large values of σ_ζ^2, spectral distortions exclude all black holes masses $M_{\rm BH} \gtrsim {\rm few} \times 10^3 M_\odot$. This conclusion is consistent with figure 2, where we compare the bounds from COBE/FIRAS with the power spectra predicted for several values of $M_{\rm BH}$. Therefore, the existence of a non-negligible abundance of primordial SMBHs requires the presence of significant non-Gaussianities in the distribution of the primordial curvature perturbations.

4 Departures from Gaussianity

For Gaussian density perturbations, constraints from spectral distortions severely limit the abundance of primordial SMBHs that could have formed in the early universe. In this case, the variance must be small in order to limit spectral distortions, while a large variance is required to generate a non-negligible abundance of PBHs. This tension could be resolved, however, if the distribution of curvature perturbations features a heavier tail than that of a Gaussian. Such non-Gaussianities thus potentially allow primordial SMBHs to form[13] without necessarily violating spectral distortion constraints.[14]

Fortunately, the distribution of primordial density perturbations is generically predicted to be non-Gaussian. Firstly, there is intrinsic non-Gaussianity that arises from the non-linear mapping between the curvature perturbation ζ and the density contrast δ, as can be seen in eq. (2.5). Thus, even if the probability distribution function for ζ were exactly Gaussian, the distribution in δ would not be. Secondly, and more crucially, large departures from Gaussianity are generically found in models which produce a local enhancement in the primordial power spectrum [82].

To quantify the degree of non-Gaussianity that would be required to generate primordial SMBHs without violating spectral distortion constraints, it is instructive to consider a class of probability distribution functions of the form [104]

$$P_\delta^{(n)} = \frac{1}{2\sqrt{2}\,\sigma_0\,\Gamma\left(1 + \frac{1}{n}\right)} \exp\left[-\left(\frac{|\delta|}{\sqrt{2}\sigma_0}\right)^n\right], \tag{4.1}$$

where n parameterizes the heaviness of the distribution's tail. The variance of the density contrast is set by the second moment of the distribution:

$$\sigma_\delta^2(\sigma_0) \equiv \int_{-\infty}^{\infty} d\delta\,\delta^2\,P_\delta^{(n)} = \frac{\sigma_0^2\,\Gamma\left(1 + \frac{3}{n}\right)}{3\Gamma\left(1 + \frac{1}{n}\right)}\ . \tag{4.2}$$

Note that for $n = 2$, this reduces to the Gaussian form of eq. (2.10) with $\sigma_0^2 = \sigma_\delta^2$. For $n = 1$ the tail falls off exponentially, while for $0 < n < 1$ it falls off even more slowly; we will refer to this class of distributions with $n < 1$ as "heavy-tailed".[15]

In figure 3, we show the shape of this class of probability distributions for various choices of n. As expected, we see that smaller n gives rise to heavier tails. This raises the question of how small n must be in order to efficiently form primordial SMBHs while keeping the

---

[13]As noted in [102], large curvature perturbations in models with heavy-tailed distributions are often type II. Such perturbations have been demonstrated to form PBHs [103], however collapse in the type II case — in particular the mass of the resultant PBH — is not completely understood.

[14]Ref. [104] proposes an alternative way to obtain the extreme statistics needed to form primordial SMBHs compatible with spectral distortion bounds. Their multi-field model results in effectively two different inflationary histories for the casually disconnected Hubble patches, with a subdominant fraction experiencing more expansion. By the δN formalism this equates to large curvature perturbations, such that these patches collapse to form PBH. Since this occurs only in a tiny fraction of patches, there is no observable generation of spectral distortions.

[15]Formally, the probability distribution P_x of a random variable x is said to be "heavy" if its tail is not exponentially bounded, $\lim_{x\to\infty} e^{\lambda x}\bar{F}(x) = \infty\,\forall\,\lambda > 0$, where $\bar{F}(x) = \int_x^\infty dx'\,P_x(x')$.
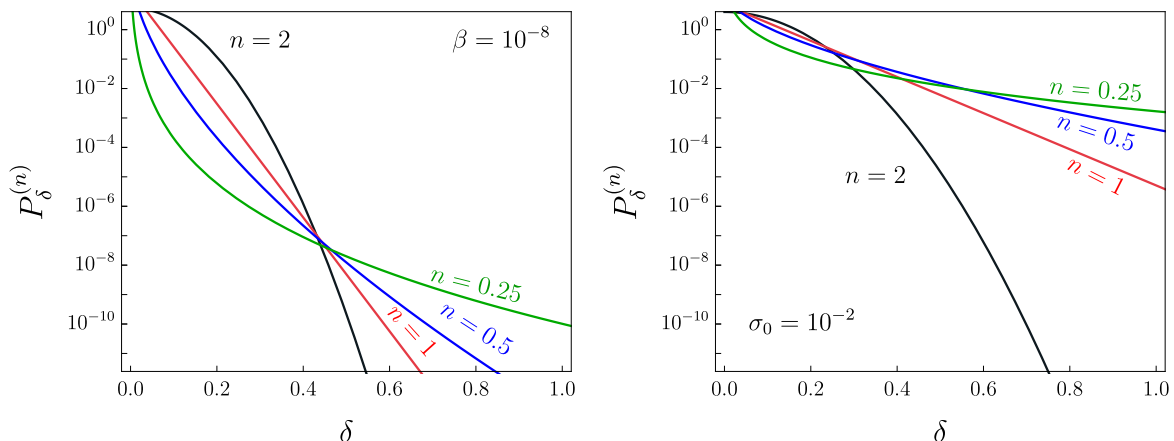
Figure 3. Probability distribution functions eq. 4.1 for various choices of n at fixed β (left) and fixed variance σ^2 (right). We see that smaller n corresponds to heavier-tailed distributions.

peak of the power spectrum within bounds of spectral distortions, $\mathcal{P}_\zeta \lesssim 10^{-4}$. In figure 4, we plot the maximum PBH mass fraction at formation β_{max}, for a variance that saturates the spectral distortion constraints from COBE/FIRAS. Note that to generate a present day abundance of $\Omega_{\mathrm{BH}} \gtrsim 10^{-20}$ with $M_{\mathrm{BH}} \lesssim 10^{11} M_\odot$, we need a heavy tail with $n \lesssim 0.6$.

We now turn to the question of what inflationary models could yield such dramatic departures from Gaussianity. In the context of single-field inflation, refs. [105–108] perturbatively studied the local non-Gaussianity that arises in models which deviate from the slow-roll attractor, as in ultra-slow-roll inflation. Going beyond perturbation theory, refs. [46, 51] used the δN formalism [109–114] to compute the non-perturbative distribution of curvature perturbations.[16] For inflaton potentials with a small step or bump-like feature that induces a period of off-attractor behavior, these studies found that the tail of the distribution can become exponential, without inducing any significant non-Gaussianities in the perturbative regime [46]. This result highlights the fact that perturbative measures of non-Gaussianity are not generally adequate to describe the large, rare fluctuations that lead to PBH formation. Finally, many of the mechanisms for enhancing local curvature perturbations rely on a temporary reduction in the inflaton's velocity. When the slow-roll classical drift vanishes, the field dynamics can receive large corrections from quantum diffusion, and the stochastic inflationary formalism [110, 116] may be necessary for a proper description of the dynamics. Combining this with the δN formalism [117], a number of studies [47, 49, 50, 118–120] have found that prominent exponential tails arise generically from quantum diffusion.

While many single-field models have been found to yield exponential tails [121], there is currently no known model which generates a heavier-tailed distribution.[17] However, as shown in figure 4, a heavy-tailed $P_\delta \sim \exp\left(-|\delta|^n\right)$ with $n \lesssim 0.6$ is needed to yield a non-negligible

---

[16]Ref. [115] presents another non-perturbative method for calculating the PBH abundance in models where ζ is related to a Gaussian reference variable ζ_G by a "generalized local transformation".

[17]Ref. [122] interprets the NANOGrav signal as evidence of PBH mergers with $M_{\mathrm{BH}} \sim 10^{11}-10^{12} M_\odot$, and claims that μ-distortion constraints can be overcome for sufficiently non-Gaussian single-field models. However they make no reference to y-type distortions, which are more constraining for this mass range, and which we have verified rule out this single-field scenario for any non-negligible abundance.
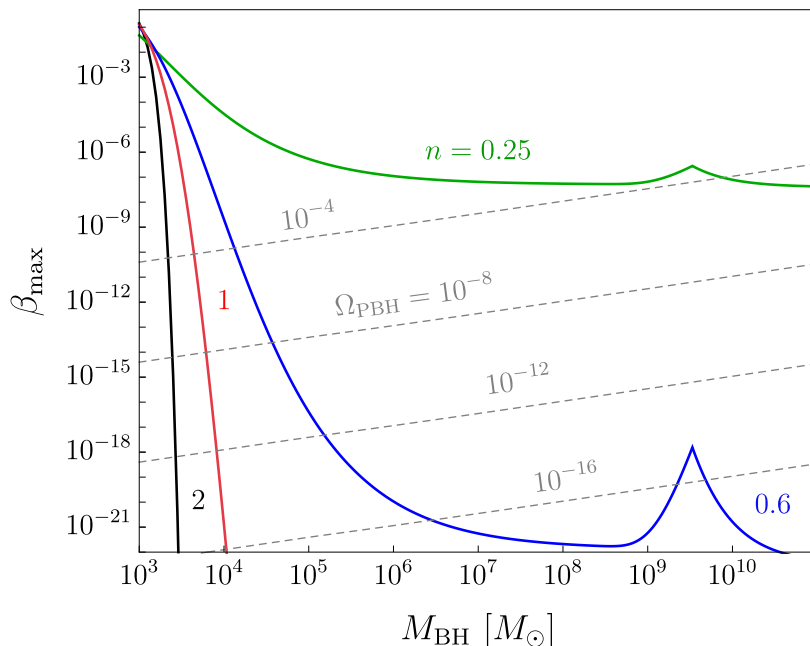
Figure 4. The maximum primordial black hole mass fraction at formation β_{max} as a function of mass M_{BH} for a value of the variance σ_ζ^2 that saturates the spectral distortion constraints from COBE/FIRAS, as estimated according to eq. (3.7). We assume the distribution function given in eq. (4.1) and consider Gaussian ($n = 2$, black), exponential ($n = 1$, red), and power law ($n = 0.6$ blue, $n = 0.25$ green) behavior in the tail. Note that the cusps which appear near $M_{\text{BH}} \sim 3 \times 10^9 \, M_\odot$ correspond to the value of M_{BH} at which μ- and y-type spectral distortions are equally restrictive. Contours of constant Ω_{BH}, as computed using eq. (2.2), are shown in dashed gray.

population of primordial SMBHs while satisfying bounds from CMB spectral distortions. While it is unclear whether primordial SMBHs can appreciably form in any viable single-field models, it is plausible that the necessary heavy tails can arise in certain multi-field scenarios. In particular, curvaton models have long been known to generate density perturbations with sizeable non-Gaussianities in the case that the curvaton remains subdominant at the time of its decay [123]. While the standard curvaton with quadratic potential is incapable of producing the dramatic non-Gaussianities needed for our scenario, there is good reason to believe that these can be augmented for a self-interacting curvaton model. We explore these possibilities in the following sections.

5   Standard curvaton scenario

Curvaton models introduce a second light, unstable spectator field that is present during inflation and that is responsible for generating the dominant contribution to the primordial curvature perturbations [124–127]. The perturbations of the curvaton are initially isocurvature, but become adiabatic upon curvaton decay sometime after inflation ends [128]. Due to the non-linearity inherent in this transfer, the full perturbation ζ can become quite non-Gaussian. In particular, when the curvaton is still very subdominant at decay, the inefficient conversion can yield a very heavy-tailed distribution for ζ.

Non-Gaussianity in the curvaton model was first investigated using the δN formalism in ref. [123], with implications for PBH formation analyzed in refs. [58, 102, 129]. As we will see, the standard curvaton model with only a quadratic potential cannot produce sufficient non-Gaussianity to generate a non-negligible abundance of SMBHs without violating spectral distortions constraints.

5.1 Curvaton cosmology

We begin by reviewing the calculation of the curvature perturbation ζ and its statistics in the standard curvaton scenario [123], for which the total potential is

$$V(\phi, \chi) = V_\phi(\phi) + V_\chi(\chi), \tag{5.1}$$

where V_ϕ is the unspecified potential of the inflaton ϕ, and $V_\chi = m_\chi^2 \chi^2/2$ is the quadratic potential of the curvaton χ. The curvaton mass is required to be light, satisfying $m_\chi \ll H$ throughout inflation, such that quantum perturbations are the dominant influence on its evolution. This also implies that the background field $\bar{\chi}$ will remain effectively fixed at some initial value $\bar{\chi}_*$ during inflation, where a star denotes the value of quantities at horizon exit. For the curvaton energy density to remain subdominant throughout inflation, we demand $\bar{\chi}_* \ll \sqrt{2V_\phi/m_\chi^2}$. Just like the inflaton, the curvaton receives perturbations $\delta\chi_* \simeq H_*/2\pi$ set by the Hubble rate at horizon exit H_*. Since the curvaton is a weakly coupled field, we expect the perturbations $\delta\chi_*$ to be described by a Gaussian random field. Thus we can write the curvaton at horizon exit as the sum of a background field and a linear perturbation, with no higher order terms:

$$\chi_* = \bar{\chi}_* + \delta\chi_*. \tag{5.2}$$

The goal of this section will be to relate these initial Gaussian field perturbations to the total curvature perturbation ζ via some mapping $\zeta = f(\delta\chi_*)$. This will be the key to constructing the probability distribution function for ζ, since the statistics of a non-Gaussian variable are completely determined by the statistics of a Gaussian reference variable when the mapping between them is specified.

When inflation ends and the inflaton decays, the universe enters into an era of radiation domination, with $\rho_R \sim a^{-4}$. At this point, the curvaton energy density is subdominant and its fluctuations are still isocurvature in nature. As the Hubble rate decreases, it eventually drops below m_χ, causing the curvaton to start oscillating about the minimum of its potential. We denote the field value at which this occurs by $\bar{\chi}_0$. During this oscillating phase, the curvaton redshifts like matter with $\rho_\chi \propto a^{-3}$ and its energy density grows linearly relative to radiation. Finally, when $H \sim \tau^{-1}$, where τ is the χ lifetime, the curvaton decays to radiation and its isocurvature perturbations become adiabatic perturbations, assuming the decay products thermalize with the existing radiation.

5.2 The δN formalism

To calculate the distribution of the curvature perturbations in this model, we employ the δN formalism [109–114, 130], which we review in appendix A. This technique identifies ζ on large scales ($k \ll aH$) with the variation of inflationary e-folds across Hubble patches and

non-perturbatively captures its non-Gaussianities. The δN formalism was first used to study non-Gaussianity in curvaton models in refs. [123, 131]. On a general hypersurface of uniform curvaton density, the conserved curvaton curvature perturbation ζ_χ is [113, 131]

$$\zeta_\chi(t, \vec{x}) = \delta N(t, \vec{x}) + \frac{1}{3} \ln \left(\frac{\rho_\chi(t, \vec{x})}{\bar{\rho}_\chi(t)} \right) , \qquad (5.3)$$

where $\delta N(t, \vec{x})$ is the perturbed number of e-folds, $\rho_\chi(t, \vec{x})$ is the χ energy density, and $\bar{\rho}_\chi(t)$ is its background value. In spatially flat slicing, this becomes

$$\zeta_\chi(t, \vec{x}) = \frac{1}{3} \ln \left(\frac{\rho_\chi(t, \vec{x})}{\bar{\rho}_\chi(t)} \right) , \qquad (5.4)$$

and the curvaton energy density can be written as

$$\rho_\chi(t, \vec{x}) = e^{3\zeta_\chi(t, \vec{x})} \bar{\rho}_\chi(t) . \qquad (5.5)$$

In uniform total density slicing, eq. (5.3) becomes

$$\zeta_\chi(t, \vec{x}) = \zeta + \frac{1}{3} \ln \left(\frac{\rho_\chi^{(u)}(t, \vec{x})}{\bar{\rho}_\chi^{(u)}(t)} \right) , \qquad (5.6)$$

where ζ is the total curvature perturbation.[18] Since ζ and ζ_χ are gauge invariant quantities, eq. (5.5) can be equated with eq. (5.6) to yield

$$\rho_\chi^{(u)}(t, \vec{x}) = e^{3(\zeta_\chi - \zeta)} \bar{\rho}_\chi^{(u)}(t) . \qquad (5.7)$$

A similar treatment for the radiation energy density in uniform total density slicing gives

$$\rho_R^{(u)}(t, \vec{x}) = e^{4(\zeta_R - \zeta)} \bar{\rho}_R^{(u)}(t) \simeq e^{-4\zeta} \bar{\rho}_R^{(u)}(t) , \qquad (5.8)$$

where we have assumed for simplicity that the main contribution to the curvature perturbation comes from the curvaton. In order to derive analytic results, we work in the instantaneous decay approximation such that the curvaton decays when $H = \tau^{-1}$, where τ is the curvaton lifetime. On a uniform total density slice at $t = \tau$, the energy densities satisfy

$$\rho_R^{(u)}(\tau, \vec{x}) + \rho_\chi^{(u)}(\tau, \vec{x}) = \bar{\rho}^{(u)}(\tau) , \qquad (5.9)$$

where $\bar{\rho}^{(u)} = \bar{\rho}_R^{(u)} + \bar{\rho}_\chi^{(u)}$ is the total homogeneous energy density. Substituting eqs. (5.7) and (5.8), this becomes a 4th degree algebraic equation for ζ at τ:

$$e^{4\zeta} - \left(e^{3\zeta_\chi} \Omega_{\chi, \tau} \right) e^\zeta + (\Omega_{\chi, \tau} - 1) = 0 . \qquad (5.10)$$

Alternatively, it is customary to introduce the parameter r_τ, defined as [124]:

$$r_\tau = \frac{3\Omega_{\chi, \tau}}{4 - \Omega_{\chi, \tau}} = \left. \frac{3\bar{\rho}_\chi^{(u)}}{3\bar{\rho}_\chi^{(u)} + 4\bar{\rho}_R^{(u)}} \right|_\tau , \qquad (5.11)$$

---

[18]Note that this generically has non-vanishing mean, $\langle \zeta \rangle \neq 0$, and so when we later consider PBH formation, we will have to define a physical $\zeta_\text{phys} \equiv \zeta - \langle \zeta \rangle$ [58]. The expectation value $\langle \zeta \rangle$ can be computed using the Gaussian P_{δ_χ} as $\langle \zeta \rangle = \int d\delta_\chi \, \zeta \, P_{\delta_\chi}$, with ζ expressed as a function of δ_χ given in eq. (5.13).

in terms of which the equation for ζ becomes:

$$e^{4\zeta} - \frac{4r_\tau}{3 + r_\tau}\left(e^{3\zeta_\chi}\right)e^\zeta + \frac{3r_\tau - 3}{3 + r_\tau} = 0\,. \tag{5.12}$$

The general solution is

$$\zeta = \ln X\,, \quad X = \frac{B^{1/2} + \sqrt{Ar_\tau B^{-1/2} - B}}{(3 + r_\tau)^{1/3}}\,, \tag{5.13}$$

where $A = e^{3\zeta_\chi}$ and we have defined

$$B = \frac{1}{2}\left[C^{1/3} + (r_\tau - 1)(3 + r_\tau)^{1/3}C^{-1/3}\right] \tag{5.14}$$

$$C = (Ar_\tau)^2 + \sqrt{(Ar_\tau)^4 + (3 + r_\tau)(1 - r_\tau)^3}\,. \tag{5.15}$$

This gives the mapping $\zeta = \ln[X(\zeta_\chi)]$ between ζ and ζ_χ.

5.3 Calculating the probability distribution

Finally, to obtain ζ_χ in terms of $\delta\chi_*$, we return to eq. (5.4), which gave the curvature perturbation in spatially flat slicing as a function of perturbed and background energy densities. For the simple quadratic potential of this model, we have $\rho_\chi(t, \vec{x}) = m_\chi^2\chi^2/2$. Expanding $\chi(t, \vec{x}) = \bar{\chi}(t) + \delta\chi(t, \vec{x})$, we can write this as

$$\rho_\chi(t, \vec{x}) = \frac{1}{2}m_\chi^2\bar{\chi}^2\left(1 + \frac{\delta\chi}{\bar{\chi}}\right)^2 = \bar{\rho}_\chi(t)(1 + \delta_\chi)^2\,, \tag{5.16}$$

where $\delta_\chi = \delta\chi/\bar{\chi}$ is the curvaton contrast in spatially flat slicing. Comparing with $\rho_\chi = e^{3\zeta_\chi}\bar{\rho}_\chi$, we see we should identify $e^{3\zeta_\chi} = (1 + \delta_\chi)^2$. Finally in order to relate the contrast δ_χ to its value at horizon exit, consider the equations of motion for χ and the perturbation $\delta\chi$:

$$\frac{d^2\bar{\chi}}{dt^2} + 3H\frac{d\bar{\chi}}{dt} + m_\chi^2\bar{\chi} = 0\,, \tag{5.17a}$$

$$\frac{d^2}{dt^2}(\delta\chi) + 3H\frac{d}{dt}(\delta\chi) + \left(\frac{k^2}{a^2} + m_\chi^2\right)\delta\chi = 0\,. \tag{5.17b}$$

On superhorizon scales $k \ll aH$ is negligible and so these reduce to the same equation. This implies $\delta\chi \sim \bar{\chi}$, such that $\delta\chi/\bar{\chi} = \delta\chi_*/\bar{\chi}_*$ and

$$A = e^{3\zeta_\chi} = (1 + \delta_\chi)^2 = \left(1 + \frac{\delta\chi_*}{\bar{\chi}_*}\right)^2\,. \tag{5.18}$$

Combining with eq. (5.13), we obtain the desired mapping between ζ and the Gaussian initial field perturbations $\delta\chi_*$. We can now use probability conservation to write

$$P_\zeta[\zeta] = P_{\delta_\chi}\left[\delta_\chi^+(\zeta)\right]\left|\frac{d\delta_\chi^+}{d\zeta}\right| + P_{\delta_\chi}\left[\delta_\chi^-(\zeta)\right]\left|\frac{d\delta_\chi^-}{d\zeta}\right|\,, \tag{5.19}$$

where P_{δ_χ} is fully determined by the Gaussian variance σ_0^2 and the roots $\delta_\chi^\pm(\zeta)$ satisfy

$$\delta_\chi^\pm = -1 \pm \sqrt{\left(\frac{3 + r_\tau}{4r_\tau}\right)e^{3\zeta} + \left(\frac{3r_\tau - 3}{4r_\tau}\right)e^{-\zeta}}\,, \tag{5.20}$$

which arise from solving eq. (5.12) and substituting eq. (5.18). In figure 5, we plot the probability distribution for the curvature perturbation as given by eq. (5.19) for a few choices of r_τ, which controls the heaviness of the tail.
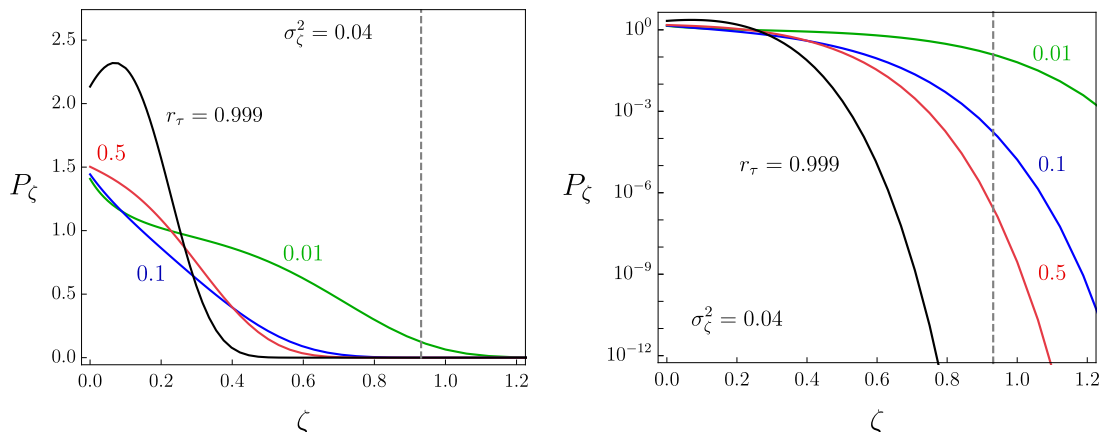
Figure 5. The probability distribution function for the curvature perturbation ζ as given by eq. (5.19) for various choices of r_τ. The vertical dashed line corresponds to the threshold value for collapse ζ_c, and the PBH mass fraction β is obtained by integrating beyond this threshold. We see that a smaller r_τ corresponds to a heavier-tailed distribution, leading to a larger PBH abundance. Note that the reference value $\sigma_\zeta^2 = 0.04$ is chosen to illustrate the heaviness of the tail as r_τ is varied, but the minimal scenario presented in section 5 cannot realize such a large value without violating the observational limits on the power spectrum shown in figure 2.

6 Heavy tails and primordial black holes in curvaton models

Viably forming an appreciable number of primordial SMBHs requires both amplified power on small scales and a departure from Gaussianity. Thus we require the following two additional ingredients:

- **Enhanced Power:** one mechanism for enhancing the power spectrum is to introduce a non-canonical kinetic term for the curvaton, which depends on the inflaton's field value [58]. In section 6.1, we review this scenario and calculate the power spectrum resulting from such a kinetic term.

- **Large Non-Gaussianity:** the non-Gaussianity in a curvaton model can be amplified through self-interactions, which lead to non-linear growth of χ perturbations between horizon exit and the onset of curvaton oscillations [132–140]. In section 6.2, we review the evolution of the non-quadratic curvaton and calculate the resulting probability distribution function.

6.1 Non-minimal curvaton scenario

The minimal curvaton model described in section 5 provides non-Gaussian statistics, but does not amplify $\mathcal{P}_\zeta$. This deficiency can be remedied with a non-canonical kinetic term[19] for the curvaton [58]:

$$\mathcal{L} \supset \frac{1}{2} f(\phi)^2 (\partial \chi)^2 \,. \tag{6.1}$$

---

[19]Such a term naturally arises in many dilatonic and axionic models of inflation [141].

If $f(\phi)$ is chosen such that this kinetic term is suppressed at field values $\phi = \phi_*$, the power spectrum will be enhanced on scales corresponding to the horizon size at ϕ_*. For concreteness, consider the evolution of the inflaton and curvaton governed by the following system of equations:

$$\ddot{\phi} + 3H\dot{\phi} + V'(\phi) = ff'\dot{\bar{\chi}}^2 \simeq 0\,, \quad \ddot{\bar{\chi}} + \left(3H + \frac{2f'}{f}\dot{\phi}\right)\dot{\bar{\chi}} + \frac{m_\chi^2}{f^2}\bar{\chi} = 0\,, \qquad (6.2)$$

where $f' \equiv \partial_\phi f$ and the source term of the first equation is negligible until the curvaton begins to oscillate. Similarly, the curvaton perturbation evolves according to

$$\frac{d^2}{dt^2}(\delta\chi) + \left(3H + \frac{2f'}{f}\dot{\phi}\right)\frac{d}{dt}(\delta\chi) + \left(\frac{k^2}{a^2} + \frac{m_\chi^2}{f^2}\right)\delta\chi \simeq 0\,, \qquad (6.3)$$

which, to leading order, can be simplified inside the horizon, $k \gg aH$, to yield

$$\frac{d^2}{dt^2}(f\delta\chi) + \frac{k^2}{a^2}(f\delta\chi) \simeq 0\,, \qquad (6.4)$$

whose solution can be written as

$$\delta\chi \simeq \frac{1}{\sqrt{2k}\,af}\exp\left(-ik\int\frac{dt}{a}\right)\,, \qquad (6.5)$$

which establishes the initial conditions in the adiabatic vacuum. As in section 5, on super-horizon scales, $k \ll aH$, $\bar{\chi}$ and $\delta\chi$ evolve according to the same equation, so their solutions have the same functional form for all $t > t_*$:

$$\frac{\delta\chi}{\bar{\chi}} = \frac{\delta\chi_*}{\bar{\chi}_*} \simeq \frac{H_*}{\sqrt{2k^3}f(\phi_*)\bar{\chi}_*}\,, \qquad (6.6)$$

where $k = a(t_*)H(t_\star)$. Using eq. (6.6), the power spectrum for $\delta\chi$ becomes

$$\mathcal{P}_{\delta_\chi}(k) = \frac{k^3}{2\pi^2}\left|\frac{\delta\chi_k}{\bar{\chi}}\right|^2 = \frac{1}{\bar{\chi}_*^2}\left(\frac{H_*}{2\pi f(\phi_*)}\right)^2\,, \qquad (6.7)$$

so, if $f(\phi)$ is chosen to have a dip at ϕ_*, corresponding to $k_* = k_{\rm BH}$, $\mathcal{P}_{\delta_\chi}$ will exhibit a peak at $k_{\rm BH}$. However, for modes far away from $k_{\rm BH}$, $f(\phi_*) \approx 1$, recovering the nearly scale-invariant spectrum required for consistency with CMB observations on larger scales. Assuming $f(\phi)$ has such a localized feature, combining eqs. (5.19), (6.7), and (2.8), the PBH abundance becomes

$$\beta = 2\int_{\delta_{\chi,c}^+}^\infty d\delta_\chi\, P_{\delta_\chi}[\delta_\chi] + 2\int_{-\infty}^{\delta_{\chi,c}^-} d\delta_\chi\, P_{\delta_\chi}[\delta_\chi] = \text{erfc}\left(\frac{\delta_{\chi,c}^+}{\sqrt{2}\sigma_0}\right) + \text{erfc}\left(\frac{|\delta_{\chi,c}^-|}{\sqrt{2}\sigma_0}\right)\,, \qquad (6.8)$$

where $\delta_{\chi,c}^\pm = \delta_\chi^\pm(\zeta_c)$ are the roots of eq. (5.20) evaluated at the threshold.

Using eq. (3.7), we obtain the maximum value of β consistent with spectral distortion constraints.[20] The degree of non-Gaussianity in this scenario is governed by r_τ, as defined in eq. (5.11). In the $r_\tau \to 1$ limit, the curvaton dominates the energy density prior to its

---

[20]Note that the variance σ_ζ^2 corresponds to the physical curvature perturbation, $\sigma_\zeta^2 = \langle\zeta_{\rm phys}^2\rangle = \langle\zeta^2\rangle - \langle\zeta\rangle^2$, which can be computed from $\zeta(\delta_\chi)$ in eq. (5.13) as $\sigma_\zeta^2 = \int d\delta_\chi\,\zeta^2\,P_{\delta_\chi} - \left(\int d\delta_\chi\,\zeta\,P_{\delta_\chi}\right)^2$.
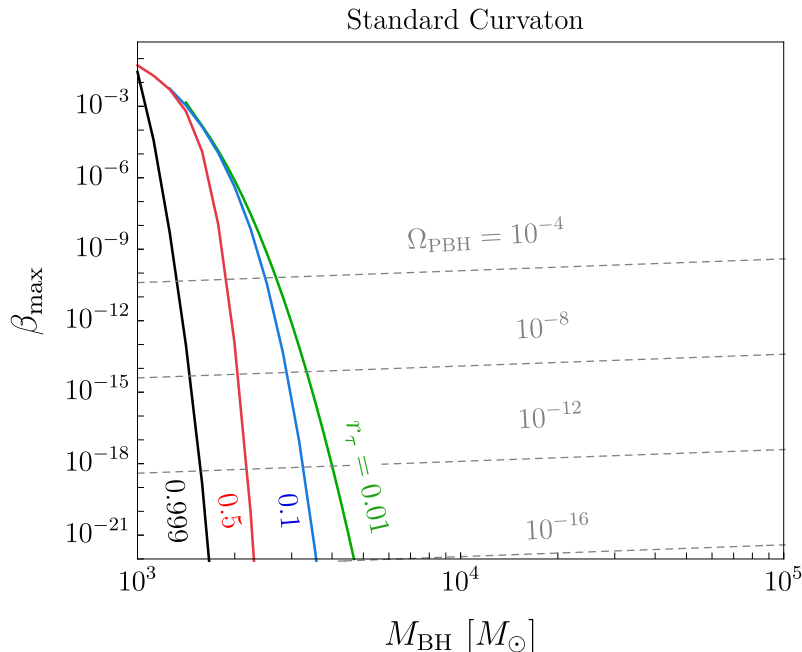
Figure 6. The maximal PBH mass fraction at formation $\beta_{\max}$ in the standard curvaton scenario for σ_ζ^2 subject to spectral distortion constraints for various choices of r_τ from eq. (5.11).

decay, so the relation between ζ and ζ_χ from eq. (5.12) is approximately linear. Thus, in this regime, the non-Gaussianity comes entirely from the non-linear relationship between ζ_χ and δ_χ; see eq. (5.18). In the opposite regime[21] that the curvaton is still very subdominant when it decays ($r_\tau \ll 1$), the relation between ζ and ζ_χ is highly non-linear, and so the degree of non-Gaussianity is large. This is reflected in figures 5 and 6. Clearly this scenario is incapable of producing primordial SMBHs while satisfying spectral distortion constraints.

6.2 Self-interacting curvaton scenario

Introducing curvaton self-interactions allows for non-linear evolution of δ_χ between horizon exit and the onset of oscillations, which can lead to even more dramatic departures from Gaussianity. This scenario is also physically well-motivated since the curvaton needs to decay for the isocurvature perturbations to be converted to adiabatic perturbations. The effects of self-interactions in curvaton models were first investigated in refs. [132–140]. However, these studies restricted themselves to computing the non-linearity parameters f_{NL} and g_{NL}, which do not capture the non-perturbative statistics in the tail of the distribution. Unfortunately following the curvaton's evolution in the non-quadratic regime and computing the exact resulting curvature distribution require extensive numerics beyond the scope of this study. We offer here a schematic picture, but leave the detailed model building to future studies.

---

[21]It may seem counterintuitive that a very subdominant curvaton can still generate the curvature perturbation. The key is that because the curvaton is subdominant during inflation, its perturbations from quantum fluctuations are large relative to the background field value. Ref. [142] finds that a subdominant curvaton can still viably produce the curvature perturbation provided $r_\tau \gtrsim 10^{-3}$.

We now allow the curvaton potential $V(\chi)$ to be an arbitrary well-defined function of χ. The cosmological evolution of the curvaton proceeds similarly to the case of the quadratic potential, but with a few crucial differences. At a time $t = t_{\text{int}}$ corresponding to $V'(\chi_*) \sim H$, χ begins rolling towards the minimum of its potential. We choose parameters such that this occurs while the curvaton's energy density is dominated by the interaction terms. At a later time $t = t_0 > t_{\text{int}}$, these interaction terms become subdominant and the curvaton mass term drives field evolution, resulting in matter-like scaling $\rho_\chi \propto a^{-3}$. Note that with self-interactions, the curvaton energy density generically falls off faster than in the quadratic case, resulting in a smaller r_τ at the time of decay.

Recall that in the case of the quadratic potential, the curvaton density contrast δ_χ remained constant after horizon exit since the background field $\bar{\chi}$ and perturbation $\delta\chi$ obeyed the same equation of motion, shown in eq. (5.17). This led to $\delta\chi/\bar{\chi} = \delta\chi_*/\bar{\chi}_*$, which allowed δ_χ to be used as a Gaussian reference variable. Upon introducing interactions this is no longer the case, as δ_χ evolves non-trivially between t_{int} and the onset of quadratic oscillations at t_0. In this regime, the equation of motion for the perturbation is:

$$\frac{d^2}{dt^2}(\delta\chi) + 3H\frac{d}{dt}(\delta\chi) + V''_\chi \delta\chi = 0 \,, \tag{6.9}$$

where it is understood that the second derivative of the potential should be evaluated at the background field value.

A natural choice of Gaussian reference variable is the initial curvaton perturbation $\delta\chi_*$, which can be related to the ζ_χ by first solving eq. (6.9) along with the equation for the background field $\bar{\chi}$, computing the total and background energy densities at decay, and finally applying eq. (5.4). The resulting $\delta\chi_*^i = g_i(\zeta_\chi)$ can then be mapped onto the total curvature perturbation ζ via eq. (5.12), since the relationship between ζ_χ and ζ is unchanged in the presence of χ self-interactions. Although an exact solution requires the use of numerical techniques, an approximate relation can be derived in the limit of weak interactions.

We are interested in the relation between $\delta\chi_*$ and ζ_χ at the time of curvaton decay. For χ values sufficiently close to the minimum of its potential, the potential is approximately quadratic, and the energy density is

$$\rho_\chi \simeq \frac{1}{2}m_\chi^2 \chi_0^2 \,, \tag{6.10}$$

where χ_0 is the amplitude at the onset of oscillations. Since non-linear evolution takes place between horizon exit and oscillation, this initial amplitude is a function of initial field value χ_*). In terms of background field values $\bar{\chi}_0 \equiv \chi_0(\bar{\chi}_*)$, this can be expanded as:

$$\chi_0 = \bar{\chi}_0 + \sum_{n=1} \frac{1}{n!}\bar{\chi}_0^{(n)}\delta\chi_*^n \,, \quad \bar{\chi}_0^{(n)} \equiv \left.\frac{\partial^n \chi_0}{\partial\chi_*^n}\right|_{\chi=\bar{\chi}_*} \,, \tag{6.11}$$

and the energy density can then be written as:

$$\rho_\chi \simeq \bar{\rho}_\chi \left[1 + \frac{1}{\bar{\chi}_0}\sum_{n=1}\frac{1}{n!}\bar{\chi}_0^{(n)}\delta\chi_*^n\right]^2 \,, \tag{6.12}$$

– 19 –

where $\bar{\rho}_\chi = \frac{1}{2} m_\chi^2 \bar{\chi}_0^2$. Comparing with eq. (5.4), the bracketed quantity is identified with $e^{3\zeta_\chi}$. Then also expanding

$$\zeta_\chi = \zeta_{\chi,1} + \sum_{n=2}^{\infty} \frac{1}{n!} \zeta_{\chi,n} \quad , \tag{6.13}$$

we can write to leading order:

$$\zeta_\chi(\delta\chi_*) = \frac{2}{3} \left(\frac{\bar{\chi}_0'}{\bar{\chi}_0} \right) \delta\chi_* + \frac{1}{3} \left(\frac{\bar{\chi}_0 \bar{\chi}_0''}{\bar{\chi}_0'^2} - 1 \right) \left(\frac{\bar{\chi}_0'}{\bar{\chi}_0} \right)^2 \delta\chi_*^2 \\ + \frac{1}{9} \left(\frac{\bar{\chi}_0^2 \bar{\chi}_0'''}{\bar{\chi}_0'^3} - 3 \frac{\bar{\chi}_0 \bar{\chi}_0''}{\bar{\chi}_0'^2} + 2 \right) \left(\frac{\bar{\chi}_0'}{\bar{\chi}_0} \right)^3 \delta\chi_*^3, \tag{6.14}$$

which can then be substituted into eq. (5.13) to obtain ζ as a function of the Gaussian reference variable $\delta\chi_*$. Note that though we have written this expression to fixed order, higher order terms can become significant in the presence of large non-Gaussianities. It is also possible to invert this mapping to obtain the roots $g_i(\zeta) = \delta\chi_*^i(\zeta)$. The probability distribution is then:

$$P_\zeta[\zeta] = \sum_j \left| \frac{g_j(\zeta)}{d\zeta} \right| P_{\delta\chi_*}[g_j(\zeta)], \tag{6.15}$$

where the sum runs over all real roots.

In figure 7, we plot the maximal PBH abundance consistent with spectral distortion constraints for a sample set of parameters. Comparison with $\beta_{\max}$ in the standard curvaton scenario (see figure 6) reveals the dramatic amplification of non-Gaussianity that self-interactions can afford. We leave the determination of a potential that could actually yield these parameter values to future investigation.

7 Discussion and conclusions

Much remains to be understood about the origin and evolution of our universe's most massive black holes. The inferred population of supermassive black holes with $M_{\rm BH} \sim 10^6 - 10^{11} M_\odot$ in the high-redshift universe is perhaps surprising, and challenges the standard assumption that these objects formed from low mass seeds which grew through the processes of accretion and mergers. In this study, we have taken this as motivation to consider the possibility that some of our universe's supermassive black holes may be primordial in origin, having formed from the direct collapse of overdensities seeded by inflation.

Forming primordial SMBH from direct collapse requires an enhanced power spectrum on small scales ($k \sim 10 - 10^4 \, \text{Mpc}^{-1}$), which results in dangerous CMB spectral distortions. Since the CMB exhibits a nearly perfect blackbody spectrum, such distortions exclude the possibility that a population of primordial SMBH could have formed from Gaussian density perturbations. However, if the distribution of primordial curvature perturbations were highly non-Gaussian, it is possible that primordial black holes may have formed from smaller peaks in the power spectrum. To evade limits from spectral distortions, the tail of the probability distribution must be very heavy, falling off as $P_\zeta \sim \exp\left(-|\zeta|^n\right)$ with $n \lesssim 0.6$; we are not aware of any single-field inflationary model that can realize this behavior.
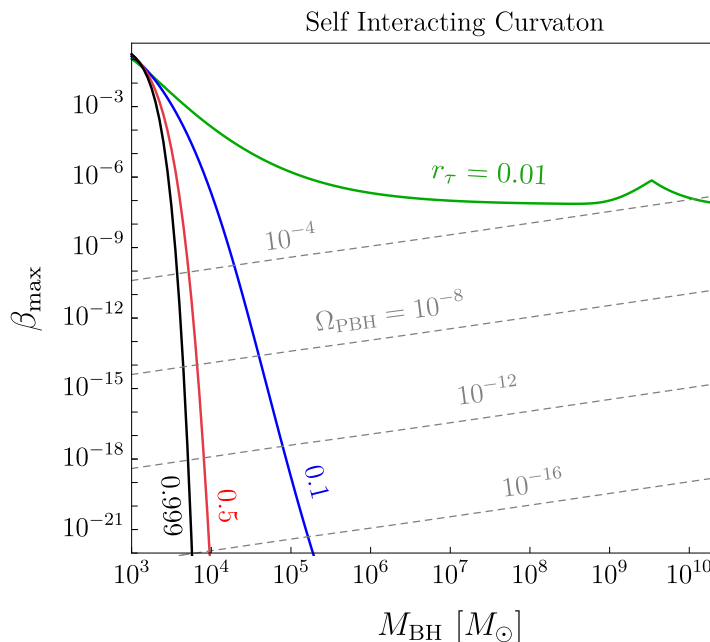
Figure 7. Maximal PBH mass fraction at formation $\beta_{\max}$ as a function of PBH mass in the self-interacting curvaton model from section 6.2, where σ_ζ^2 saturates spectral distortion bounds for different values of r_τ, as defined in eq. (5.11). We take $\zeta_\chi = c_1\,\delta\chi_* + c_2\,\delta\chi_*^2 + c_3\,\delta\chi_*^3$ to take the form of eq. (6.14), with sample parameters fixed as $(c_1, c_2, c_3) = (1, 0.5, 0.1)$. Contours of constant Ω_{BH} today are shown in dashed gray.

In this paper, we have explored the possibility of generating curvature perturbations with heavy-tailed probability distributions in the event that a self-interacting curvaton field is also present as a spectator during inflation. In the standard curvaton scenario, non-Gaussianity arises from the inefficient conversion of isocurvature perturbations into adiabatic perturbations when the curvaton decays. However, the degree of non-Gaussianity in this minimal realization is insufficient to yield an appreciable primordial SMBH population. Introducing curvaton self-interactions results in non-linear evolution of the curvaton contrast δ_χ between horizon exit and the onset of quadratic oscillations, potentially resulting in a heavier-tailed distribution, as seen in figure 7. We leave the detailed model building and determination of a potential that can realize this benchmark point to future investigation. Provided such a potential can be found, the non-minimal self-interacting curvaton could viably yield SMBHs from the direct collapse of primordial perturbations, without violating spectral distortion constraints.

We note that beyond the bounds from CMB spectral distortions, there are two further more speculative constraints that potentially need to be addressed in a full model. First, as pointed out by ref. [143], the small scale curvature perturbation impacts structure evolution as traced by dark matter halos. Presuming a bump in the small scale power spectrum, they investigated host halo and subhalo evolution. By comparing the results of their simulations with the observed number of dwarf spheroidal galaxies and stellar streams, they were able to place bounds on $\mathcal{P}_\zeta$ to greater sensitivity than COBE/FIRAS for a region of wavenumbers. The result would exclude some, but not all, of the SMBH mass range we consider. These

bounds are less robust than those coming from CMB spectral distortion and are subject to modeling uncertainties, but nevertheless should be noted. Second, the large non-Gaussianities described in this model would likely lead to heavy clustering of quasars. Ref. [144] calculated the observed angular correlation function using the 92 quasars at $z \sim 6$ reported by the Subaru High-z Exploration of Low-Luminosity Quasars project and compared this with that predicted in a PBH model which used a light spectator field to source non-Gaussian primordial perturbations. They found the amplitude of the angular correlation function predicted by the model to be much larger than that observed, a result which would seem to preclude PBHs as the sole progenitors of SMBHs in this redshift range. More concretely, they were able to restrict the fraction of PBH originating SMBHs to $\lesssim 10^{-4}$.

These potential constraints notwithstanding, this work is especially timely in light of two distinct recent observations. The James Webb Space Telescope (JWST) has reported a number of surprisingly luminous high-redshift galaxy candidates [145–148] whose existence poses a challenge to the standard ΛCDM paradigm. These massive early galaxies could conceivably be explained if primordial black holes accelerated galaxy formation in the early universe [149]. Meanwhile, the NANOGrav collaboration and several other pulsar timing array experiments have just announced evidence of a signal consistent with the stochastic gravitational wave background in the nHz frequency range [150–153]. The leading astrophysical interpretation of this signal is that it consists of gravitational waves from supermassive black hole binary mergers. However, some aspects of this data, such as the frequency scaling of the spectral density parameter, are not particularly well-fit by this interpretation [154, 155]. Given that the distribution of SMBH binaries would be different if these objects were of a primordial origin, one avenue for future investigation would be to compute the gravitational wave signal predicted in this scenario. While for homogenously distributed primordial SMBHs this possibility is in conflict with constraints on total abundance from large scale structure and the UV galaxy luminosity function [156], a highly clustered population could still viably source the gravitational wave signal [157]. Given that a clustered population can arise in the presence of non-Gaussianities, it would be interesting to see what our model predicts in this context; see refs. [144, 158] for closely related work. There are also other signals, such as scalar-induced secondary gravitational waves, which could offer complimentary evidence of this scenario and deserve further study; see refs. [159, 160] for a potential connection between scalar-induced gravitational waves and the PTA signal. Regardless, these recent observations provide us with strong motivation to better understand the cosmic origin of our universe's supermassive black holes.

Acknowledgments

A The δN formalism

A.1 Review

The δN formalism [109–114, 130] is a technique for computing the non-linear curvature perturbation ζ on large scales by identifying it with the perturbed logarithmic expansion from some initial state to a final state of fixed energy density. In a homogenous background, the number of e-folds elapsed between two moments of times t_1 and t_2 is

$$\bar{N}(t_2, t_1) = \int_{t_1}^{t_2} dt\, H\,. \tag{A.1}$$

Meanwhile, the amount of expansion in a perturbed universe is [113]

$$N(t_2, t_1; \vec{x}) = \int_{t_1}^{t_2} dt\, (H + \dot{\psi})\,, \tag{A.2}$$

where ψ is the curvature perturbation appearing in the decomposition of the spatial 3-metric $g_{ij} = a^2(t)e^{2\psi(t,\vec{x})}\delta_{ij}$.[22] Note that this expression holds on superhorizon scales, where spatial gradients can be neglected. We define $\delta N \equiv N(t_2, t_1; x) - \bar{N}(t_2, t_1)$ to be the difference between the perturbed and unperturbed expansion, and see that it equates to the change in the curvature perturbation from an initial hypersurface at t_1 to a final hypersurface at t_2

$$\delta N \equiv N(t_2, t_1; \vec{x}) - \bar{N}(t_2, t_1) = \psi(t_2, \vec{x}) - \psi(t_1, \vec{x})\,. \tag{A.3}$$

Equivalently, the change in ψ going from one choice of slicing to another is the difference between the actual number of e-folds N and the homogenous background value $\bar{N}$.

Since the curvature perturbation ψ is a gauge-dependent quantity, whose value depends on the choice of slicing, it is convenient to combine this with the gauge-dependent density perturbation $\delta\rho$ to form the gauge-invariant curvature perturbation [161]:

$$\zeta(t, \vec{x}) = \psi(t, \vec{x}) + \frac{1}{3}\int_{\bar{\rho}(t)}^{\rho(t,\vec{x})} \frac{d\rho}{(1+w)\rho}\,, \tag{A.4}$$

where w is the equation of state of the cosmological fluid, $\rho(t, \vec{x})$ is the inhomogenous local energy density, and $\bar{\rho}(t)$ is the homogenous background energy density. It was demonstrated in ref. [113] that this quantity is conserved on superhorizon scales.

We would like to equate this gauge-invariant, conserved curvature perturbation ζ with the perturbed logarithmic expansion δN. By choosing the initial hypersurface at t_1 to be spatially flat, such that $\psi(t_1, \vec{x}) = 0$, from eq. (A.3) we can equate $\delta N(t_2, t_1; \vec{x} = \psi(t_2, \vec{x})$. By choosing the finial hypersurface at t_2 to be uniform density, such that $\rho(t_2, \vec{x}) = \bar{\rho}(t_2)$, from eq. (A.4) we have $\zeta(t_2, \vec{x}) = \psi(t_2, \vec{x})$. Combining these expressions gives the δN formula

$$\zeta(t_2, \vec{x}) = \delta N(t_2, t_1; \vec{x})\,, \tag{A.5}$$

relating the curvature perturbation with the perturbed expansion between a spatially flat and uniform energy density hypersurface.

---

[22]We ignore tensor perturbations.

A.2 Numerical implementation

It is also possible to implement the δN formalism numerically. Following inflaton decay, the exact system of equations describing the evolution of the curvaton and radiation bath is

$$\ddot{\chi} + \left(3H + \frac{1}{\tau}\right)\dot{\chi} + V_\chi' = 0\,, \qquad \dot{\rho}_R + 4H\rho_R = \frac{\dot{\chi}^2}{\tau}\,, \qquad H^2 = \frac{8\pi}{3M_{\rm Pl}^2}(\rho_R + \rho_\chi)\,. \qquad \text{(A.6)}$$

We set the initial conditions at the end of inflation by specifying $\chi_i = \chi_*$, $\dot{\chi}_i = 0$, and $H_i = H_*$, which in turn determines $\rho_{R,i} = \frac{3M_{\rm Pl}^2}{8\pi}H_i^2 - V_\chi(\chi_i)$. The system of equations should be evolved until a final time t_f satisfying $H_f \ll \tau^{-1}$, such that the curvaton has decayed completely. The number of e-folds elapsed is then computed as $N = \ln(a_f/a_i)$. This procedure should then be repeated for the perturbed field value $\chi_* + \delta\chi_*$, with the fluctuation determined by the size of Hubble at horizon exit $\delta\chi_* = H_*/2\pi$. Evolving until the same final hypersurface of fixed energy density, the curvature perturbation is computed as:

$$\zeta = N(\chi_* + \delta\chi_*) - N(\chi_*)\,. \qquad \text{(A.7)}$$

Repeating for many different $\delta\chi_*$ gives a functional relation between ζ and the Gaussian $\delta\chi_*$. We leave an in-depth numerical study to future investigation.

References

[1] Y. Shen et al., *A Catalog of Quasar Properties from SDSS DR7*, *Astrophys. J. Suppl.* **194** (2011) 45 [arXiv:1006.5178] [INSPIRE].

[2] E. Bañados et al., *An 800-million-solar-mass black hole in a significantly neutral Universe at redshift 7.5*, *Nature* **553** (2018) 473 [arXiv:1712.01860] [INSPIRE].

[3] N.P. Ross and N.J.G. Cross, *The near and mid-infrared photometric properties of known redshift $z \geq 5$ quasars*, *Mon. Not. Roy. Astron. Soc.* **494** (2020) 789 [arXiv:1906.06974].

[4] C.J. Willott et al., *The Canada-France High-z Quasar Survey: nine new quasars and the luminosity function at redshift 6*, *Astron. J.* **139** (2010) 906 [arXiv:0912.0281] [INSPIRE].

[5] E. Bañados et al., *The Pan-STARRS1 distant $z > 5.6$ quasar survey: more than 100 quasars within the first Gyr of the universe*, *Astrophys. J. Suppl.* **227** (2016) 11 [arXiv:1608.03279] [INSPIRE].

[6] L. Jiang et al., *The Final SDSS High-Redshift Quasar Sample of 52 Quasars at $z > 5.7$*, *Astrophys. J.* **833** (2016) 222 [arXiv:1610.05369] [INSPIRE].

[7] DES et al. collaborations, *Eight new luminous $z \geq 6$ quasars discovered via SED model fitting of VISTA, WISE and Dark Energy Survey Year 1 observations*, *Mon. Not. Roy. Astron. Soc.* **468** (2017) 4702 [arXiv:1701.04852] [INSPIRE].

[8] Y. Matsuoka et al., *Subaru High-z Exploration of Low-luminosity Quasars (SHELLQs). X. Discovery of 35 Quasars and Luminous Galaxies at $5.7 \leq z \leq 7.0$*, *Astrophys. J.* **883** (2019) 183 [arXiv:1908.07910].

[9] J. Yang et al., *Filling in the Quasar Redshift Gap at $z \sim 5.5$ II: A Complete Survey of Luminous Quasars in the Post-Reionization Universe*, arXiv:1810.11927.

[10] F. Wang et al., *Exploring Reionization-era Quasars. III. Discovery of 16 Quasars at* $6.4 \lesssim z \lesssim 6.9$ *with DESI Legacy Imaging Surveys and the UKIRT Hemisphere Survey and Quasar Luminosity Function at* $z \sim 6.7$, *Astrophys. J.* **884** (2019) 30 [arXiv:1810.11926].

[11] B. Mutlu-Pakdil, M.S. Seigar and B.L. Davis, *The local black hole mass function derived from the* $m_{BH} - p$ *and the* $m_{BH} - n$ *relations*, *Astrophys. J.* **830** (2016) 117.

[12] F. Shankar, D.H. Weinberg and J. Miralda-Escudé, *Accretion-Driven Evolution of Black Holes: Eddington Ratios, Duty Cycles, and Active Galaxy Fractions*, *Mon. Not. Roy. Astron. Soc.* **428** (2013) 421 [arXiv:1111.3574] [INSPIRE].

[13] X. Shen et al., *The bolometric quasar luminosity function at* $z = 0-7$, *Mon. Not. Roy. Astron. Soc.* **495** (2020) 3252 [arXiv:2001.02696] [INSPIRE].

[14] A. Sicilia et al., *The Black Hole Mass Function across Cosmic Time. II. Heavy Seeds and (Super)Massive Black Holes*, *Astrophys. J.* **934** (2022) 66 [arXiv:2206.07357] [INSPIRE].

[15] N. Banik, J.C. Tan and P. Monaco, *The Formation of Supermassive Black Holes from Population III.1 Seeds. I. Cosmic Formation Histories and Clustering Properties*, *Mon. Not. Roy. Astron. Soc.* **483** (2019) 3592 [arXiv:1608.04421] [INSPIRE].

[16] E.E. Salpeter, *Accretion of Interstellar Matter by Massive Objects*, *Astrophys. J.* **140** (1964) 796 [INSPIRE].

[17] SDSS collaboration, *A Survey of* $z > 5.8$ *quasars in the Sloan Digital Sky Survey I: Discovery of three new quasars and the spatial density of luminous quasars at* $z \sim 6$, *Astron. J.* **122** (2001) 2833 [astro-ph/0108063] [INSPIRE].

[18] D.J. Mortlock et al., *A luminous quasar at a redshift of* $z = 7.085$, *Nature* **474** (2011) 616 [arXiv:1106.6088] [INSPIRE].

[19] X.-B. Wu et al., *An ultraluminous quasar with a twelve-billion-solar-mass black hole at redshift 6.30*, *Nature* **518** (2015) 512 [arXiv:1502.07418] [INSPIRE].

[20] B. Trakhtenbrot, H. Netzer, P. Lira and O. Shemmer, *Black-Hole Mass and Growth Rate at* $z \simeq 4.8$: *A Short Episode of Fast Growth Followed by Short Duty Cycle Activity*, *Astrophys. J.* **730** (2011) 7 [arXiv:1012.1871] [INSPIRE].

[21] M. Volonteri, *Formation of Supermassive Black Holes*, *Astron. Astrophys. Rev.* **18** (2010) 279 [arXiv:1003.4404] [INSPIRE].

[22] Z. Haiman, *Constraints from gravitational recoil on the growth of supermassive black holes at high redshift*, *Astrophys. J.* **613** (2004) 36 [astro-ph/0404196] [INSPIRE].

[23] S.L. Shapiro, *Spin, accretion and the cosmological growth of supermassive black holes*, *Astrophys. J.* **620** (2005) 59 [astro-ph/0411156] [INSPIRE].

[24] M. Volonteri and M.J. Rees, *Quasars at* $z = 6$: *The survival of the fittest*, *Astrophys. J.* **650** (2006) 669 [astro-ph/0607093] [INSPIRE].

[25] T. Tanaka and Z. Haiman, *The Assembly of Supermassive Black Holes at High Redshifts*, *Astrophys. J.* **696** (2009) 1798 [arXiv:0807.4702] [INSPIRE].

[26] M. Volonteri, M. Habouzit and M. Colpi, *The origins of massive black holes*, *Nature Rev. Phys.* **3** (2021) 732 [arXiv:2110.10175] [INSPIRE].

[27] W. Massonneau, M. Volonteri, Y. Dubois and R.S. Beckmann, *How the super-Eddington regime regulates black hole growth in high-redshift galaxies*, *Astron. Astrophys.* **670** (2023) A180 [arXiv:2201.08766] [INSPIRE].

[28] H. Netzer, *The Largest black holes and the most luminous galaxies*, *Astrophys. J. Lett.* **583** (2003) L5 [astro-ph/0210548] [INSPIRE].

[29] P. Natarajan and E. Treister, *Is there an upper limit to black hole masses?*, *Mon. Not. Roy. Astron. Soc.* **393** (2009) 838 [arXiv:0808.2813] [INSPIRE].

[30] K. Inayoshi and Z. Haiman, *Is there a maximum mass for black holes in galactic nuclei?*, *Astrophys. J.* **828** (2016) 110 [arXiv:1601.02611].

[31] M. Kawasaki, A. Kusenko and T.T. Yanagida, *Primordial seeds of supermassive black holes*, *Phys. Lett. B* **711** (2012) 1 [arXiv:1202.3848] [INSPIRE].

[32] J.L. Bernal, A. Raccanelli, L. Verde and J. Silk, *Signatures of primordial black holes as seeds of supermassive black holes*, *JCAP* **05** (2018) 017 [*Erratum ibid.* **01** (2020) E01] [arXiv:1712.01311] [INSPIRE].

[33] A. Smith, V. Bromm and A. Loeb, *The first supermassive black holes*, *Astron. Geophys.* **58** (2017) 3.22.

[34] J. Liu et al., *Primordial black hole production during first-order phase transitions*, *Phys. Rev. D* **105** (2022) L021303 [arXiv:2106.05637] [INSPIRE].

[35] J. Garriga, A. Vilenkin and J. Zhang, *Black holes and the multiverse*, *JCAP* **02** (2016) 064 [arXiv:1512.01819] [INSPIRE].

[36] H. Davoudiasl, P.B. Denton and J. Gehrlein, *Supermassive Black Holes, Ultralight Dark Matter, and Gravitational Waves from a First Order Phase Transition*, *Phys. Rev. Lett.* **128** (2022) 081101 [arXiv:2109.01678] [INSPIRE].

[37] H.-L. Huang et al., *Supermassive primordial black holes in multiverse: for nano-Hertz gravitational wave and high-redshift JWST galaxies*, arXiv:2306.17577 [INSPIRE].

[38] B.J. Carr, *The Primordial black hole mass spectrum*, *Astrophys. J.* **201** (1975) 1 [INSPIRE].

[39] S.M. Leach, M. Sasaki, D. Wands and A.R. Liddle, *Enhancement of superhorizon scale inflationary curvature perturbations*, *Phys. Rev. D* **64** (2001) 023512 [astro-ph/0101406] [INSPIRE].

[40] J. Garcia-Bellido and E. Ruiz Morales, *Primordial black holes from single field models of inflation*, *Phys. Dark Univ.* **18** (2017) 47 [arXiv:1702.03901] [INSPIRE].

[41] C. Germani and T. Prokopec, *On primordial black holes from an inflection point*, *Phys. Dark Univ.* **18** (2017) 6 [arXiv:1706.04226] [INSPIRE].

[42] G. Ballesteros and M. Taoso, *Primordial black hole dark matter from single field inflation*, *Phys. Rev. D* **97** (2018) 023501 [arXiv:1709.05565] [INSPIRE].

[43] M.P. Hertzberg and M. Yamada, *Primordial Black Holes from Polynomial Potentials in Single Field Inflation*, *Phys. Rev. D* **97** (2018) 083509 [arXiv:1712.09750] [INSPIRE].

[44] S.S. Mishra and V. Sahni, *Primordial Black Holes from a tiny bump/dip in the Inflaton potential*, *JCAP* **04** (2020) 007 [arXiv:1911.00057] [INSPIRE].

[45] K. Inomata, E. McDonough and W. Hu, *Amplification of primordial perturbations from the rise or fall of the inflaton*, *JCAP* **02** (2022) 031 [arXiv:2110.14641] [INSPIRE].

[46] Y.-F. Cai et al., *Highly non-Gaussian tails and primordial black holes from single-field inflation*, *JCAP* **12** (2022) 034 [arXiv:2207.11910] [INSPIRE].

[47] C. Pattison, V. Vennin, H. Assadullahi and D. Wands, *Quantum diffusion during inflation and primordial black holes*, *JCAP* **10** (2017) 046 [arXiv:1707.00537] [INSPIRE].

[48] M. Biagetti, G. Franciolini, A. Kehagias and A. Riotto, *Primordial Black Holes from Inflation and Quantum Diffusion*, *JCAP* **07** (2018) 032 [arXiv:1804.07124] [INSPIRE].

[49] J.M. Ezquiaga, J. García-Bellido and V. Vennin, *The exponential tail of inflationary fluctuations: consequences for primordial black holes*, *JCAP* **03** (2020) 029 [arXiv:1912.05399] [INSPIRE].

[50] C. Pattison, V. Vennin, D. Wands and H. Assadullahi, *Ultra-slow-roll inflation with quantum diffusion*, *JCAP* **04** (2021) 080 [arXiv:2101.05741] [INSPIRE].

[51] Y.-F. Cai et al., *One small step for an inflaton, one giant leap for inflation: A novel non-Gaussian tail and primordial black holes*, *Phys. Lett. B* **834** (2022) 137461 [arXiv:2112.13836] [INSPIRE].

[52] J. Garcia-Bellido, A.D. Linde and D. Wands, *Density perturbations and black hole formation in hybrid inflation*, *Phys. Rev. D* **54** (1996) 6040 [astro-ph/9605094] [INSPIRE].

[53] S. Clesse and J. García-Bellido, *Massive Primordial Black Holes from Hybrid Inflation as Dark Matter and the seeds of Galaxies*, *Phys. Rev. D* **92** (2015) 023524 [arXiv:1501.07565] [INSPIRE].

[54] A.R. Brown, *Hyperbolic Inflation*, *Phys. Rev. Lett.* **121** (2018) 251601 [arXiv:1705.03023] [INSPIRE].

[55] G.A. Palma, S. Sypsas and C. Zenteno, *Seeding primordial black holes in multifield inflation*, *Phys. Rev. Lett.* **125** (2020) 121301 [arXiv:2004.06106] [INSPIRE].

[56] J. Fumagalli, S. Renaux-Petel, J.W. Ronayne and L.T. Witkowski, *Turning in the landscape: A new mechanism for generating primordial black holes*, *Phys. Lett. B* **841** (2023) 137921 [arXiv:2004.08369] [INSPIRE].

[57] M. Braglia et al., *Generating PBHs and small-scale GWs in two-field models of inflation*, *JCAP* **08** (2020) 001 [arXiv:2005.02895] [INSPIRE].

[58] S. Pi and M. Sasaki, *Primordial black hole formation in nonminimal curvaton scenarios*, *Phys. Rev. D* **108** (2023) L101301 [arXiv:2112.12680] [INSPIRE].

[59] S.R. Geller, W. Qin, E. McDonough and D.I. Kaiser, *Primordial black holes from multifield inflation with nonminimal couplings*, *Phys. Rev. D* **106** (2022) 063535 [arXiv:2205.04471] [INSPIRE].

[60] O. Özsoy and G. Tasinato, *Inflation and Primordial Black Holes*, *Universe* **9** (2023) 203 [arXiv:2301.03600] [INSPIRE].

[61] Y. Cai, M. Zhu and Y.-S. Piao, *Primordial black holes from null energy condition violation during inflation*, arXiv:2305.10933 [INSPIRE].

[62] PLANCK collaboration, *Planck 2018 results. VI. Cosmological parameters*, *Astron. Astrophys.* **641** (2020) A6 [*Erratum ibid.* **652** (2021) C4] [arXiv:1807.06209] [INSPIRE].

[63] J.C. Mather et al., *Measurement of the Cosmic Microwave Background spectrum by the COBE FIRAS instrument*, *Astrophys. J.* **420** (1994) 439 [INSPIRE].

[64] D.J. Fixsen et al., *The Cosmic Microwave Background spectrum from the full COBE FIRAS data set*, *Astrophys. J.* **473** (1996) 576 [astro-ph/9605054] [INSPIRE].

[65] PLANCK collaboration, *Planck 2018 results. IX. Constraints on primordial non-Gaussianity*, *Astron. Astrophys.* **641** (2020) A9 [arXiv:1905.05697] [INSPIRE].

[66] PLANCK collaboration, *Planck 2018 results. X. Constraints on inflation*, *Astron. Astrophys.* **641** (2020) A10 [arXiv:1807.06211] [INSPIRE].

[67] J.M. Bardeen, J.R. Bond, N. Kaiser and A.S. Szalay, *The Statistics of Peaks of Gaussian Random Fields*, *Astrophys. J.* **304** (1986) 15 [ɪɴSPIRE].

[68] A.M. Green, A.R. Liddle, K.A. Malik and M. Sasaki, *A New calculation of the mass fraction of primordial black holes*, *Phys. Rev. D* **70** (2004) 041502 [astro-ph/0403181] [ɪɴSPIRE].

[69] S. Young and M. Musso, *Application of peaks theory to the abundance of primordial black holes*, *JCAP* **11** (2020) 022 [arXiv:2001.06469] [ɪɴSPIRE].

[70] C.-M. Yoo, T. Harada, S. Hirano and K. Kohri, *Abundance of Primordial Black Holes in Peak Theory for an Arbitrary Power Spectrum*, *PTEP* **2021** (2021) 013E02 [arXiv:2008.02425] [ɪɴSPIRE].

[71] A.D. Gow, C.T. Byrnes, P.S. Cole and S. Young, *The power spectrum on small scales: Robust constraints and comparing PBH methodologies*, *JCAP* **02** (2021) 002 [arXiv:2008.03289] [ɪɴSPIRE].

[72] W.H. Press and P. Schechter, *Formation of galaxies and clusters of galaxies by selfsimilar gravitational condensation*, *Astrophys. J.* **187** (1974) 425 [ɪɴSPIRE].

[73] M. Shibata and M. Sasaki, *Black hole formation in the Friedmann universe: Formulation and computation in numerical relativity*, *Phys. Rev. D* **60** (1999) 084002 [gr-qc/9905064] [ɪɴSPIRE].

[74] A. Escrivà, C. Germani and R.K. Sheth, *Universal threshold for primordial black hole formation*, *Phys. Rev. D* **101** (2020) 044022 [arXiv:1907.13311] [ɪɴSPIRE].

[75] V. Atal, J. Cid, A. Escrivà and J. Garriga, *PBH in single field inflation: the effect of shape dispersion and non-Gaussianities*, *JCAP* **05** (2020) 022 [arXiv:1908.11357] [ɪɴSPIRE].

[76] V. Atal, J. Garriga and A. Marcos-Caballero, *Primordial black hole formation with non-Gaussian curvature perturbations*, *JCAP* **09** (2019) 073 [arXiv:1905.13202] [ɪɴSPIRE].

[77] C.-M. Yoo, J.-O. Gong and S. Yokoyama, *Abundance of primordial black holes with local non-Gaussianity in peak theory*, *JCAP* **09** (2019) 033 [arXiv:1906.06790] [ɪɴSPIRE].

[78] A. Kehagias, I. Musco and A. Riotto, *Non-Gaussian Formation of Primordial Black Holes: Effects on the Threshold*, *JCAP* **12** (2019) 029 [arXiv:1906.07135] [ɪɴSPIRE].

[79] B. Carr, S. Clesse, J. García-Bellido and F. Kühnel, *Cosmic conundra explained by thermal history and primordial black holes*, *Phys. Dark Univ.* **31** (2021) 100755 [arXiv:1906.08217] [ɪɴSPIRE].

[80] I. Musco, K. Jedamzik and S. Young, *Primordial black hole formation during the QCD phase transition: threshold, mass distribution and abundance*, arXiv:2303.07980 [ɪɴSPIRE].

[81] T. Harada, C.-M. Yoo and K. Kohri, *Threshold of primordial black hole formation*, *Phys. Rev. D* **88** (2013) 084051 [*Erratum ibid.* **89** (2014) 029903] [arXiv:1309.4201] [ɪɴSPIRE].

[82] G. Ferrante, G. Franciolini, J.A. Iovino and A. Urbano, *Primordial non-Gaussianity up to all orders: Theoretical aspects and implications for primordial black hole models*, *Phys. Rev. D* **107** (2023) 043520 [arXiv:2211.01728] [ɪɴSPIRE].

[83] V. De Luca, A. Kehagias and A. Riotto, *How well do we know the primordial black hole abundance: The crucial role of nonlinearities when approaching the horizon*, *Phys. Rev. D* **108** (2023) 063531 [arXiv:2307.13633] [ɪɴSPIRE].

[84] S. Young, C.T. Byrnes and M. Sasaki, *Calculating the mass fraction of primordial black holes*, *JCAP* **07** (2014) 045 [arXiv:1405.7023] [ɪɴSPIRE].

[85] K. Ando, K. Inomata and M. Kawasaki, *Primordial black holes and uncertainties in the choice of the window function*, *Phys. Rev. D* **97** (2018) 103528 [arXiv:1802.06393] [ɪɴSPIRE].

[86] S. Young, *The primordial black hole formation criterion re-examined: Parametrisation, timing and the choice of window function*, *Int. J. Mod. Phys. D* **29** (2019) 2030002 [arXiv:1905.01230] [InSPIRE].

[87] R.A. Sunyaev and Y.B. Zeldovich, *Small scale fluctuations of relic radiation*, *Astrophys. Space Sci.* **7** (1970) 3.

[88] Y.B. Zeldovich and R.A. Sunyaev, *The Interaction of Matter and Radiation in a Hot-Model Universe*, *Astrophys. Space Sci.* **4** (1969) 301 [InSPIRE].

[89] A.F. Illarionov and R.A. Sunyaev, *Why the number of galactic X-ray stars is so small?*, *Astron. Astrophys.* **39** (1975) 185 [InSPIRE].

[90] W. Hu and J. Silk, *Thermalization and spectral distortions of the cosmic background radiation*, *Phys. Rev. D* **48** (1993) 485 [InSPIRE].

[91] J. Chluba, A.L. Erickcek and I. Ben-Dayan, *Probing the inflaton: Small-scale power spectrum constraints from measurements of the CMB energy spectrum*, *Astrophys. J.* **758** (2012) 76 [arXiv:1203.2681] [InSPIRE].

[92] R. Khatri and R.A. Sunyaev, *Beyond y and μ: the shape of the CMB spectral distortions in the intermediate epoch,* $1.5 \times 10^4 < z < 2 \times 10^5$, *JCAP* **09** (2012) 016 [arXiv:1207.6654] [InSPIRE].

[93] J. Chluba and R.A. Sunyaev, *Superposition of blackbodies and the dipole anisotropy: A Possibility to calibrate CMB experiments*, *Astron. Astrophys.* **424** (2003) 389 [astro-ph/0404067] [InSPIRE].

[94] A. Stebbins, *CMB Spectral Distortions from the Scattering of Temperature Anisotropies*, astro-ph/0703541 [InSPIRE].

[95] J. Chluba and R.A. Sunyaev, *The evolution of CMB spectral distortions in the early Universe*, *Mon. Not. Roy. Astron. Soc.* **419** (2012) 1294 [arXiv:1109.6552] [InSPIRE].

[96] C. Pitrou and A. Stebbins, *Parameterization of temperature and spectral distortions in future CMB experiments*, *Gen. Rel. Grav.* **46** (2014) 1806 [arXiv:1402.0968] [InSPIRE].

[97] B.J. Carr and J.E. Lidsey, *Primordial black holes and generalized constraints on chaotic inflation*, *Phys. Rev. D* **48** (1993) 543 [InSPIRE].

[98] J. Chluba, *Which spectral distortions does ΛCDM actually predict?*, *Mon. Not. Roy. Astron. Soc.* **460** (2016) 227 [arXiv:1603.02496] [InSPIRE].

[99] A.M. Green and B.J. Kavanagh, *Primordial Black Holes as a dark matter candidate*, *J. Phys. G* **48** (2021) 043001 [arXiv:2007.10722] [InSPIRE].

[100] S. Bird, H.V. Peiris, M. Viel and L. Verde, *Minimally Parametric Power Spectrum Reconstruction from the Lyman-alpha Forest*, *Mon. Not. Roy. Astron. Soc.* **413** (2011) 1717 [arXiv:1010.1519] [InSPIRE].

[101] C.T. Byrnes, P.S. Cole and S.P. Patil, *Steepest growth of the power spectrum and primordial black holes*, *JCAP* **06** (2019) 028 [arXiv:1811.11158] [InSPIRE].

[102] A.D. Gow, T. Miranda and S. Nurmi, *Primordial black holes from a curvaton scenario with strongly non-Gaussian perturbations*, *JCAP* **11** (2023) 006 [arXiv:2307.03078] [InSPIRE].

[103] M. Kopp, S. Hofmann and J. Weller, *Separate Universes Do Not Constrain Primordial Black Hole Formation*, *Phys. Rev. D* **83** (2011) 124025 [arXiv:1012.4369] [InSPIRE].

[104] T. Nakama, T. Suyama and J. Yokoyama, *Supermassive black holes formed by direct collapse of inflationary perturbations*, *Phys. Rev. D* **94** (2016) 103522 [arXiv:1609.02245] [InSPIRE].

[105] M.H. Namjoo, H. Firouzjahi and M. Sasaki, *Violation of non-Gaussianity consistency relation in a single field inflationary model*, *EPL* **101** (2013) 39001 [arXiv:1210.3692] [INSPIRE].

[106] X. Chen, H. Firouzjahi, M.H. Namjoo and M. Sasaki, *A Single Field Inflation Model with Large Local Non-Gaussianity*, *EPL* **102** (2013) 59001 [arXiv:1301.5699] [INSPIRE].

[107] X. Chen et al., *In-in and δN calculations of the bispectrum from non-attractor single-field inflation*, *JCAP* **12** (2013) 039 [arXiv:1308.5341] [INSPIRE].

[108] Y.-F. Cai et al., *Revisiting non-Gaussianity from non-attractor inflation models*, *JCAP* **05** (2018) 012 [arXiv:1712.09998] [INSPIRE].

[109] D.S. Salopek and J.R. Bond, *Nonlinear evolution of long wavelength metric fluctuations in inflationary models*, *Phys. Rev. D* **42** (1990) 3936 [INSPIRE].

[110] A.A. Starobinsky, *Dynamics of Phase Transition in the New Inflationary Universe Scenario and Generation of Perturbations*, *Phys. Lett. B* **117** (1982) 175 [INSPIRE].

[111] M. Sasaki and E.D. Stewart, *A General analytic formula for the spectral index of the density perturbations produced during inflation*, *Prog. Theor. Phys.* **95** (1996) 71 [astro-ph/9507001] [INSPIRE].

[112] M. Sasaki and T. Tanaka, *Superhorizon scale dynamics of multiscalar inflation*, *Prog. Theor. Phys.* **99** (1998) 763 [gr-qc/9801017] [INSPIRE].

[113] D.H. Lyth, K.A. Malik and M. Sasaki, *A General proof of the conservation of the curvature perturbation*, *JCAP* **05** (2005) 004 [astro-ph/0411220] [INSPIRE].

[114] D.H. Lyth and Y. Rodriguez, *The Inflationary prediction for primordial non-Gaussianity*, *Phys. Rev. Lett.* **95** (2005) 121302 [astro-ph/0504045] [INSPIRE].

[115] A.D. Gow et al., *Non-perturbative non-Gaussianity and primordial black holes*, *EPL* **142** (2023) 49001 [arXiv:2211.08348] [INSPIRE].

[116] A.A. Starobinsky, *Stochastic de Sitter (Inflationary) Stage in the Early Universe*, *Lect. Notes Phys.* **246** (1986) 107 [INSPIRE].

[117] V. Vennin and A.A. Starobinsky, *Correlation Functions in Stochastic Inflation*, *Eur. Phys. J. C* **75** (2015) 413 [arXiv:1506.04732] [INSPIRE].

[118] Y. Tada and V. Vennin, *Statistics of coarse-grained cosmological fields in stochastic inflation*, *JCAP* **02** (2022) 021 [arXiv:2111.15280] [INSPIRE].

[119] H. Firouzjahi, A. Nassiri-Rad and M. Noorbala, *Stochastic Ultra Slow Roll Inflation*, *JCAP* **01** (2019) 040 [arXiv:1811.02175] [INSPIRE].

[120] A. Achucarro, S. Cespedes, A.-C. Davis and G.A. Palma, *The hand-made tail: non-perturbative tails from multifield inflation*, *JHEP* **05** (2022) 052 [arXiv:2112.14712] [INSPIRE].

[121] S. Pi and M. Sasaki, *Logarithmic Duality of the Curvature Perturbation*, *Phys. Rev. Lett.* **131** (2023) 011002 [arXiv:2211.13932] [INSPIRE].

[122] V. Atal, A. Sanglas and N. Triantafyllou, *NANOGrav signal as mergers of Stupendously Large Primordial Black Holes*, *JCAP* **06** (2021) 022 [arXiv:2012.14721] [INSPIRE].

[123] M. Sasaki, J. Valiviita and D. Wands, *Non-Gaussianity of the primordial perturbation in the curvaton model*, *Phys. Rev. D* **74** (2006) 103003 [astro-ph/0607627] [INSPIRE].

[124] D.H. Lyth and D. Wands, *Generating the curvature perturbation without an inflaton*, *Phys. Lett. B* **524** (2002) 5 [hep-ph/0110002] [INSPIRE].

[125] T. Moroi and T. Takahashi, *Effects of cosmological moduli fields on cosmic microwave background*, *Phys. Lett. B* **522** (2001) 215 [hep-ph/0110096] [INSPIRE].

[126] K. Enqvist and M.S. Sloth, *Adiabatic CMB perturbations in pre-big bang string cosmology*, *Nucl. Phys. B* **626** (2002) 395 [hep-ph/0109214] [INSPIRE].

[127] N. Bartolo and A.R. Liddle, *The Simplest curvaton model*, *Phys. Rev. D* **65** (2002) 121301 [astro-ph/0203076] [INSPIRE].

[128] S. Mollerach, *Isocurvature Baryon Perturbations and Inflation*, *Phys. Rev. D* **42** (1990) 313 [INSPIRE].

[129] S. Young and C.T. Byrnes, *Primordial black holes in non-Gaussian regimes*, *JCAP* **08** (2013) 052 [arXiv:1307.4995] [INSPIRE].

[130] D. Langlois, F. Vernizzi and D. Wands, *Non-linear isocurvature perturbations and non-Gaussianities*, *JCAP* **12** (2008) 004 [arXiv:0809.4646] [INSPIRE].

[131] N. Bartolo, S. Matarrese and A. Riotto, *On nonGaussianity in the curvaton scenario*, *Phys. Rev. D* **69** (2004) 043503 [hep-ph/0309033] [INSPIRE].

[132] K. Enqvist and T. Takahashi, *Signatures of Non-Gaussianity in the Curvaton Model*, *JCAP* **09** (2008) 012 [arXiv:0807.3069] [INSPIRE].

[133] K. Enqvist, S. Nurmi, O. Taanila and T. Takahashi, *Non-Gaussian Fingerprints of Self-Interacting Curvaton*, *JCAP* **04** (2010) 009 [arXiv:0912.4657] [INSPIRE].

[134] K. Enqvist et al., *The Subdominant Curvaton*, *JCAP* **11** (2009) 003 [arXiv:0906.3126] [INSPIRE].

[135] O. Taanila, *Primordial Perturbations from a Self-interacting Curvaton*, Ph.D. thesis, Helsinki University, Helsinki, Finland (2010) [INSPIRE].

[136] K. Enqvist, *The self-interacting curvaton*, *Prog. Theor. Phys. Suppl.* **190** (2011) 62 [arXiv:1012.1711] [INSPIRE].

[137] C.T. Byrnes, K. Enqvist and T. Takahashi, *Scale-dependence of Non-Gaussianity in the Curvaton Model*, *JCAP* **09** (2010) 026 [arXiv:1007.5148] [INSPIRE].

[138] J. Fonseca and D. Wands, *Non-Gaussianity and Gravitational Waves from Quadratic and Self-interacting Curvaton*, *Phys. Rev. D* **83** (2011) 064025 [arXiv:1101.1254] [INSPIRE].

[139] C.T. Byrnes, K. Enqvist, S. Nurmi and T. Takahashi, *Strongly scale-dependent polyspectra from curvaton self-interactions*, *JCAP* **11** (2011) 011 [arXiv:1108.2708] [INSPIRE].

[140] T. Kobayashi and T. Takahashi, *Runnings in the Curvaton*, *JCAP* **06** (2012) 004 [arXiv:1203.3011] [INSPIRE].

[141] G. Domènech and M. Sasaki, *Conformal Frame Dependence of Inflation*, *JCAP* **04** (2015) 022 [arXiv:1501.07699] [INSPIRE].

[142] K. Enqvist et al., *The Subdominant Curvaton*, *JCAP* **11** (2009) 003 [arXiv:0906.3126] [INSPIRE].

[143] S. Ando, N. Hiroshima and K. Ishiwata, *Constraining the primordial curvature perturbation using dark matter substructure*, *Phys. Rev. D* **106** (2022) 103014 [arXiv:2207.05747] [INSPIRE].

[144] T. Shinohara et al., *Supermassive primordial black holes: A view from clustering of quasars at $z \sim 6$*, *Phys. Rev. D* **108** (2023) 063510 [arXiv:2304.08153] [INSPIRE].

[145] R.P. Naidu et al., *Two remarkably luminous galaxy candidates at $z \approx 10-12$ revealed by JWST*, *Astrophys. J. Lett.* **940** (2022) L14 [`arXiv:2207.09434`].

[146] N.J. Adams et al., *Discovery and properties of ultra-high redshift galaxies ($9 < z < 12$) in the JWST ERO SMACS 0723 Field*, *Mon. Not. Roy. Astron. Soc.* **518** (2023) 4755 [`arXiv:2207.11217`].

[147] I. Labbe et al., *A very early onset of massive galaxy formation*, `arXiv:2207.12446`.

[148] S.L. Finkelstein et al., *Ceers key paper. I. An early look into the first 500 Myr of galaxy formation with JWST*, *Astrophys. J. Lett.* **946** (2023) L13 [`arXiv:2211.05792`].

[149] G. Hütsi et al., *Did JWST observe imprints of axion miniclusters or primordial black holes?*, *Phys. Rev. D* **107** (2023) 043502 [`arXiv:2211.02651`] [InSPIRE].

[150] NANOGRAV collaboration, *The NANOGrav 15 yr Data Set: Evidence for a Gravitational-wave Background*, *Astrophys. J. Lett.* **951** (2023) L8 [`arXiv:2306.16213`] [InSPIRE].

[151] EPTA and InPTA: collaborations, *The second data release from the European Pulsar Timing Array — III. Search for gravitational wave signals*, *Astron. Astrophys.* **678** (2023) A50 [`arXiv:2306.16214`] [InSPIRE].

[152] D.J. Reardon et al., *Search for an Isotropic Gravitational-wave Background with the Parkes Pulsar Timing Array*, *Astrophys. J. Lett.* **951** (2023) L6 [`arXiv:2306.16215`] [InSPIRE].

[153] H. Xu et al., *Searching for the Nano-Hertz Stochastic Gravitational Wave Background with the Chinese Pulsar Timing Array Data Release I*, *Res. Astron. Astrophys.* **23** (2023) 075024 [`arXiv:2306.16216`] [InSPIRE].

[154] NANOGRAV collaboration, *The NANOGrav 15 yr Data Set: Bayesian Limits on Gravitational Waves from Individual Supermassive Black Hole Binaries*, *Astrophys. J. Lett.* **951** (2023) L50 [`arXiv:2306.16222`] [InSPIRE].

[155] NANOGRAV collaboration, *The NANOGrav 15 yr Data Set: Constraints on Supermassive Black Hole Binaries from the Gravitational-wave Background*, *Astrophys. J. Lett.* **952** (2023) L37 [`arXiv:2306.16220`] [InSPIRE].

[156] Y. Gouttenoire, S. Trifinopoulos, G. Valogiannis and M. Vanvlasselaer, *Scrutinizing the Primordial Black Holes Interpretation of PTA Gravitational Waves and JWST Early Galaxies*, `arXiv:2307.01457` [InSPIRE].

[157] P.F. Depta, K. Schmidt-Hoberg, P. Schwaller and C. Tasillo, *Do pulsar timing arrays observe merging primordial black holes?*, `arXiv:2306.17836` [InSPIRE].

[158] T. Shinohara, T. Suyama and T. Takahashi, *Angular correlation as a novel probe of supermassive primordial black holes*, *Phys. Rev. D* **104** (2021) 023526 [`arXiv:2103.13692`] [InSPIRE].

[159] G. Franciolini, J.A. Iovino, V. Vaskonen and H. Veermae, *Recent Gravitational Wave Observation by Pulsar Timing Arrays and Primordial Black Holes: The Importance of Non-Gaussianities*, *Phys. Rev. Lett.* **131** (2023) 201401 [`arXiv:2306.17149`] [InSPIRE].

[160] S. Wang, Z.-C. Zhao, J.-P. Li and Q.-H. Zhu, *Implications of Pulsar Timing Array Data for Scalar-Induced Gravitational Waves and Primordial Black Holes: Primordial Non-Gaussianity f_{NL} Considered*, `arXiv:2307.00572` [InSPIRE].

[161] J.M. Bardeen, *Gauge Invariant Cosmological Perturbations*, *Phys. Rev. D* **22** (1980) 1882 [InSPIRE].